Effectiveness of Dental Masks and an Industrial Mask to Filter Aerodynamically Respirable Dust Particles Created by Grinding Dental Composite Adhesives

M.S. Candidate: Devan R Vest DDS

A Thesis submitted to the Department of Orthodontics and
The Advanced Education Committee of the
Oregon Health & Science University
School of Dentistry
In partial fulfillment of the requirements
For the degree of
Master of Science

November 2009

Effectiveness of Dental Masks and an Industrial Mask to Filter Aerodynamically Respirable Dust Particles Created by Grinding Dental Composite Adhesives

A thesis presented by Devan R. Vest

In partial fulfillment for the degree of Master of Science in Orthodontics

December 2009

[redacted]

Jack L. Ferracane, Ph.D.

Professor and Chairman

Department of Restorative Dentistry

[redacted]

David A. Covell, Jr., Ph.D., D.D.S.

Associate Professor and Chairman

Department of Orthodontics

[redacted]

Larry M. Doyle, D.D.S.

Associate Professor and Graduate Program Director

Department of Orthodontics

Table of Contents

Abstract:

Introduction: Quartz has been cited by the International Agency for Research on Cancer (IARC) as a human carcinogen. Exposure to quartz containing aerodynamically respirable aerosols (particle size of 0.5-5.0 μm) is possible during air rotary abrasion to remove the adhesive from teeth following orthodontic bracket debond. A previous study (Almeida, 2006) characterized the particle size distribution of composite adhesive dust within an aerosol generated by air-rotary abrasion of quartz filled adhesives using an 8-stage impactor device (Cascade Impactor, Tisch, Cleves, OH). The purpose of this study was to: 1) determine the effectiveness of dental masks in removing aerodynamically respirable dust (0.5 – 5.0 μm) created by grinding dental composite adhesives and 2) determine the effectiveness and accuracy of the 8-stage impactor in filtering and separating dust particles according to size fractions. **Methods:** Quartz-containing composite adhesive Transbond XT (3M Unitek) was abraded into an aerosol using high speed air-rotary abrasion, and separated into size fractions using an 8-stage Cascade Impactor. Separate trials using three different masks [1-Kimberly-Clark Tecnol Procedure Mask (Kimberly-Clark, Roswell, Georgia); 2-Kimberly-Clark Tecnol Cone Mask (Kimberly-Clark Worldwide, Inc., Roswell, Georgia); 3-3M Particulate Respirator N95(3M Occupational Health and Environmental Safety Division, model #8214, St. Paul, Minnesota)] placed over the intake orifice of the air sampler were conducted using Transbond XT. For the second part of the study, the Cascade Impactor used in the experiment was tested for accuracy, using particles of known sizes and a Microtrac S3500 laser particle analyzer.

Results: The results showed that at least 5% of the total dust generated was potentially aerodynamically respirable (particle size of 0.5 μm – 5 μm). The procedure mask filtered significantly more particles than the cone mask. The cone mask allowed 1-2.5% of the particles generated to pass, while the procedure mask allowed 0.03-0.06% of the particles generated to pass through to the impactor stages. When compared to controls, the procedure mask reduced the collected dust mass by over 99%, while the cone mask reduced the collected dust mass by 84%. The N95 mask was the only mask that completely blocked all particles from entering the impactor. Of the total particles collected in the impactor, at least 19.1% of the particles by mass were aerodynamically

respirable when the procedure mask was used, as compared with at least 39.1% of the particles when the cone mask was used. According to the Microtrac S3500 particle analyzer, approximately 95% of the particles were less than or equal to 1.1 μm, while the 8-stage impactor shows that approximately 46% of the particles were less than or equal to 1.1 μm when comparing the same sample. **Conclusion:** The 8-stage Cascade Impactor is unable to accurately separate the particles into the appropriate size fractions. Exposure to aerodynamically respirable dust containing quartz particles appears likely during removal of Transbond orthodontic adhesive with a high-speed handpiece. The results showed that use of a dental mask does not completely protect operators from exposure to particles smaller than 5 μm, which are the greatest risk for inhalation to deeper regions of the lungs. The procedure dental mask performed much better than the cone dental mask at filtering particles, while the N95 mask was able to filter 100% of the particles generated. Further studies are needed to determine the extent of this exposure in clinical settings.

Introduction:

Bonding of brackets to teeth using composite adhesives has been the standard of practice in the orthodontic profession for decades. In order to provide clinically adequate bond strength, some of the composites rely upon the use of quartz as a filler (Collard et al., 1991). Of potential concern, quartz has been recognized by the International Agency for Research on Cancer (IARC) as a human carcinogen, and can be responsible for the deadly lung disease, silicosis (IARC 1997). Silicosis is characterized by a nodular pulmonary fibrosis throughout the lungs (Hunter 1955). These pathologic changes generally take years if not decades to occur following exposure.

One of the easiest and most effective means of removing composite adhesive following orthodontic bracket debonding is with air-rotary abrasion using a high-speed handpiece (Ireland et al., 2003). This procedure generates a dust aerosol that is spread throughout the work environment (Harrel and Molinari, 2004). Within this aerosol, dusts particles between 0.5μm – 5μm have the ability to travel to the lung's terminal alveoli without being filtered out in the upper respiratory tract (Giordano 2000). Particles in this size range have been termed aerodynamically respirable (Collard et al., 1991; Giordano, 2000). Therefore exposure to these particles may place orthodontic operators at risk to develop pulmonary pathology.

The use of universal precautions such as the dental mask is commonly thought to protect operators from this type of exposure (Brune and Beltesbredde, 1980b). However studies suggest that dental masks filter out only about 70% of the dust mass under ideal circumstances (Brune and Beltesbredde, 1980a; Korn and Ndhlovu, 1989; Collard et al., 1991; Harrel and Molinari, 2004). This indicates that reliance on dental masks alone may not provide complete protection from aerodynamically respirable exposure.

This project had two purposes. The first aim was to determine the effectiveness of masks (both dental and industrial) in removing aerodynamically respirable orthodontic adhesive dust generated by air rotary abrasion. The second aim was to determine the effectiveness and accuracy of the 8-stage non-viable cascade impactor air sampler in filtering and separating respirable dust according to particle size. The hypothesis for each aim respectively is that 1) dental masks provide little protection from aerodynamically respirable dust when filtering the particles from sampled air, and 2) using an 8-stage non-viable cascade impactor air sampler, aerodynamically respirable dust can be isolated accurately according to particle size.

Background and Significance:

The use of composite adhesives to bond orthodontic brackets to teeth has become nearly universal throughout the world. These composites are very similar to the types of composites used in restorative dentistry. They all contain a resin component based on dimethacrylates, mainly Bis-GMA (bisphenol A diglycidylether methacrylate). They also contain a reinforcing filler component that is generally a hard substance such as amorphous silica, crystalline silica or some type of radiopaque glass, i.e. aluminosilicate glass. Finally, some sort of chemical or photoactive initiator is used to promote curing of the composite. These can be benzoyl peroxide / tertiary amine for chemical activation or in the case of photoactivation, the radical generator is champhoroquinone coupled with an amine accelerator. The main difference between the restorative and orthodontic composites is their formulation. Based on required strength, adhesion to tooth, and no requirement for high polishability, orthodontic composites generally use larger filler particles of around 1-5 μm, and are reinforced to the extent of 70% by mass. This is different from restorative composites which generally use smaller, submicron particles and a variety of filler levels depending on the composite's intended function (Collard 1989; Collard et al., 1991; Ireland et al., 2003).

During orthodontic debonding, brackets are removed using a peeling motion, inducing bond failure at the interface between the bracket and the composite adhesive. The adhesive that remains bonded to the tooth can then be removed with instruments such as hand scalers, ultrasonic scalers, or with air rotary abrasion. Air rotary abrasion is the most common and efficient means of composite removal and can be accomplished using either high or slow-speed handpieces (Ireland et al., 2003). Although effective, the process generates aerosols that can accumulate dust on the operator's gloves, patient's

face, operatory equipment, and into the surrounding air. This aerosol can be spread for a distance of at least 18 inches (Harrel and Molinari, 2004). The air-driven high-speed handpiece is second only to ultrasonic cleaners in generation of airborne contaminants (Miller and Micik, 1978). Further, from a bacterial standpoint, air abrasion generates environmental bacterial counts that nearly equal those generated by ultrasonic scalers (Harrel and Molinari, 2004).

Greco and Lai (2008) introduced a new method of assessing aerosolized bacteria generated during orthodontic debonding procedures. A collection system was used to harvest bonding dust liberated during debonding. Three commercial masks were tested to see whether they provide protection from the aerosol. In the study, twenty-one species of oral bacteria were identified including Propionibacterium acnes (causes uveitis and enophthalmitis) and Actinomyces viscosus (one of several species causing actinomycosis). In addition, the two dental masks tested offered no protection against the aerosolized bacteria. Only the N-95 Industrial mask (95% filtration rate at 0.3 μm) offered sufficient protection against aerosolized bacteria.

In two research articles, Collard and co-workers (1989; 1991) introduced dentistry to what in the environmental hygiene industry is called *aerodynamically respirable* dust. They took restorative composites, ground them with high-speed air-rotary abrasion, and analyzed the dust. Aerodynamically respirable dust is the term used to describe any aerosol which contains particles that are within the 0.5-5.0 μm size range (Giordano, 2000). Dust in this size range has the potential to be biologically dangerous. Because the particles are so small, they are easily maintained in the airstream over long distances, thus bypassing the body's built-in filtering mechanisms. Larger particles are mainly deposited in the upper respiratory tract and upper bronchioles of the lung where alveolar

macrophages and mucociliary elevator mechanisms can efficiently remove them from the lungs (Reiser and Last, 1979). Particles between 0.5-5.0 μm in size, however, are likely to be deposited in the terminal, non-ciliated alveoli (Collard et al., 1991, Harrel and Molinari, 2004). Here the body depends almost entirely on macrophages to consume and clear any debris. In most cases this mechanism is sufficient, but as has been shown with asbestos inhalation the processes can be ineffective. The asbestos particles induce fibrotic changes in the lungs that can lead to respiratory failure and cancer in the form of mesothelioma (Collard et al., 1989).

As mentioned previously, some orthodontic adhesives use silica as a filler material. Silica has three crystalline forms; quartz, cristobalite, and tridymite (Donaldson et al., 1992). All of these forms have been recognized by the International Agency for Research on Cancer as a group I human carcinogen (IARC, 1997). It has also been recognized as a human carcinogen by the National Toxicology Program (NTP, 2000). When aerodynamically respirable crystalline silica is inhaled, it can cause damage to the pulmonary tissues. This inflammation tissue can be converted in time into collagenous scars, which can cause permanent constriction and deformities of bronchi and bronchioles (Gross et al., 1970). Ultimately, this can lead to a debilitating and deadly form of pneumoconiosis (pulmonary fibrogenic disease associated with the inhalation of dusts) called silicosis (Hearl, 1997).

Silicosis is characterized by a nodular pulmonary fibrosis throughout the lungs (Hunter, 1955). These pathologic changes generally take years if not decades to occur following exposure. The chronic nature and need for long term exposure may explain why little attention has been paid to this disease in the dental and orthodontic literature. Industrial hygiene groups have long since recognized the potential hazards of silica on

the human lung (Wozniak et al., 1979; Dufrensne et al., 1987; Luchtel et al., 1989; Hearl, 1997; Bello et al., 2002; Linch, 2002; Yabuta and Ohta, 2003). It is possible that the clinical dental community has not been using these materials in dentistry for a sufficient length of time to observe widespread pathology, or under normal conditions they have not reached exposure levels large enough to cause disease.

Three factors that affect pathogenicity of silica are microstructure, particle size, and concentration (Collard et al., 1991). Silica is found in either an amorphous or a crystalline form (Dufresne et al., 1987). The crystalline form has been found to be the more pathogenic. Tridymite is the most fibrogenic, followed by cristobalite and quartz (Reiser and Last, 1979). The exact mechanism of pathology is not known. Studies suggest that it may be due to negative surface charges on the dust particles (Horvath, 1976; Wallace et al., 1990). Others suggest that the shape of the crystal can cause physical damage to the cells they encounter (Soutar et al., 1983). The size of the particles also can greatly influence pathogenicity. Particles in the range of 0.5 to 5 μm can make their way into terminal alveoli where removal is solely dependent on macrophage clearance (Reiser and Last, 1979; Collard et al., 1989; Giordano, 2000). It is in these terminal alveoli that the fibrogenic changes are initiated leading to pulmonary constriction. Reiser and Last (1976) suggests that particles between 1.0 and 2.0 μm are the most fibrogenic. Concentration and length of exposure will also act to determine if the disease will be acute or chronic.

Acute silicosis occurs when large doses of aerodynamically respirable aerosols are inhaled over a short period of time. Death in these cases usually occurs in 1-2 years due to progressive respiratory failure. There is no effective treatment in these cases (Reiser and Last, 1976). Although this type of exposure is unlikely in a typical

orthodontic or dental setting, chronic exposure can lead to a similar disease called chronic silicosis. Chronic silicosis develops as a result of frequent, low dose exposures to silica. The threshold exposure is usually measured as a concentration ratio of silicon/sulfur in the pulmonary tissues. When the Si/S ratio exceeds 0.3, clear-cut pulmonary changes are imminent (Funahashi et al., 1984). Until this occurs, the disease may remain entirely asymptomatic, even for decades. In industries where the risk of silica inhalation has been highly recognized such as mining, tunneling, and brick making, routine pulmonary radiographic tests are generally taken. Workers may go for years without any radiographic or respiratory function changes. Only when the characteristic fibrotic nodules develop within the lungs will the pulmonary changes become noticeable on chest x-rays. A slowly progressive constriction of the respiratory pathway with loss of function ensues. As in the acute case, management is directed solely at alleviating symptoms (Reiser and Last, 1976).

Another concern is that non-aerodynamically respirable dust may also present a health concern. Because the nose and upper respiratory tracts will likely filter out these larger mass particles, they will not contribute to lung pathology. However, Bello et al. (2002) believes they may contribute to elevated cancers of the buccal cavity, throat, and GI tract. Further, several epidemiologic studies have implicated the ingestion of silica as a cause of esophageal cancer (Rose, 1968a,b; O'Neill et al., 1980, 1982; Newman, 1986). As the upper respiratory tract filters higher sized dust particles, they are generally cleared from the body through ingestion. As a result, a reported 2.8-fold risk increase in esophageal cancer along with a clear dose-response by length of exposure has been found in industries where silica dust inhalation is common (Pan et al., 1999).

There is also a theory called *particle toxicity*, which states that inhaled particles can have adverse health effects irrespective of chemical composition. For example, titanium dioxide dust has a low biological toxicity and is considered inert. However, large doses of it have been shown to cause failure of lung clearance, chronic inflammation and fibrosis, and a few cancers in rats (Lee et al., 1983). What is unclear is whether or not humans respond with equally susceptibility. What must be kept in mind is that pneumoconiosis has been documented from a wide range of occupationally exposed dusts. This is supported by Gross et al. (1970), who found pulmonary changes induced by "safe" material dusts such as glass, ceramic aluminum silicate (an alternative to asbestos fibers), and brucite (magnesium hydroxide). These dusts induced the mobilization of macrophages, which consumed the dust and occupied alveolar spaces. This in turn evaginated off respiratory bronchioles and alveolar ducts. The walls of these alveoli were thickened by a combination of surface cell enlargement and arborescence of the septal argyrophilic stroma. This further led to the development of fibroblastic tissue processes. In time these areas were resolved, but it opened questions as to the effects of repeated insults and the long term responses of the alveolar tissues. Although silicosis may not develop as a result of respirable dust exposure, partial pulmonary impairment might be a more likely consequence of chronic respirable dust inhalation.

The link between silica and pulmonary fibrosis leading to cancer appears at first to be reasonably clear-cut. However, it should be pointed out that not all research is in agreement. Soutar et al. (2000) has eloquently compared various studies and points out the strengths and faults of each. He brings to light that the role of silica in the development of lung pathology may not be as direct as we believe it to be. Most interesting is the study done by Davis et al. (1983), where occupational dust exposures in

Vermont granite workers were examined. The study included extremely detailed records of dust and quartz measurements, as well as a series of cross-sectional surveys. He concluded that there was no relationship between silica exposure and lung cancer. It should be noted that this study commenced in the 1920's and it required conversions from particle counts to gravimetric measurements. This caused large errors in exposure estimates and weakened the power of the study. A second study of British coal miners from the 1950's also found no relation between silica exposure and lung cancer (Miller et al., 1998). It should be noted that in this study silica content in the respirable dust was less than 10%. No data was given as to whether or not this silica was free or bound to other components within the dust. Finally, Gross et al. (1979) pointed out that rats inhaling 100 mg/m^3 of fibrous glass for more than a year did not produce any proliferative lesions.

In regard to the dental literature, the group that has received most of the concern regarding hazardous exposure to respirable dental and orthodontic materials has been on laboratory technicians (Mjor, 1985). It has been generally believed that high-volume evacuation systems as well as the use of dental facemasks protect orthodontic operators from the hazards of airborne dusts. The typical high-volume system used in clinical practices has an aperture diameter of 0.95 cm and an air displacement of 10 standard cubic feet per minute (scfm). This is equivalent to 4.72 liters per minute (L/m). By definition, this does not classify as high-volume evacuation (HVE; Harrel and Molinari, 2004). Brune and Beltesbredde (1980b) determined that an effective evacuation system should have an aperture diameter of 3.5 cm and an air displacement of 30 L/m to effectively remove respirable dust. Even at this rate research suggests that only 90% of contamination is removed (Harrel and Molinari, 2004). This difference suggests that the

air displacement and dust removal of a typical orthodontic evacuation system is at most only 16% of what is considered adequate (Collard et al., 1991).

In a study by Oberg and Brosseau (2008), 9 surgical masks were tested for their ability to filter monodisperse latex sphere aerosols (0.895, 2.0, and 3.1μm) as well as sodium chloride particles (0.075 μm) at 84 L/min. The 9 masks showed a wide range of penetration for both the monodisperse latex sphere aerosols (0-84% penetration) and sodium chloride particles (4-90% penetration). The dental masks used in the study showed significantly higher average penetration (53-90%) when compared to those used in hospital settings (4-37%) for both the monodisperse latex sphere aerosols (6-75% compared to 0.02-0.7%) and the sodium chloride particles (53-90% compared to 4-37%).

The facemask traditionally worn by dental clinicians may give a false sense of protection from respirable dusts. Brune and Beltesbredde (1980b) pointed out that the three-dimensional network structure of the dental facemask constitutes a pore size ranging from 10 to 100 μm. This will reduce inhaled dust in some cases by only 70% based on weight, allowing particles in the critical size range of 0.5 to 5.0 μm to pass unimpeded through the mask (Brune and Beltesbredde, 1980b). In essence, the masks that the dental industry relies on for protection are only equivalent to a coarse-dust mask used in the mining industry. Thus clinicians are poorly protected and are at significant risk from breathing respirable silica under the circumstances commonly found in most clinical settings (Korn and Ndhlovu, 1989).

The Andersen design cascade impactors, such as the one used in this study, have been widely used in the pharmaceutical industry to evaluate aerodynamic size distribution profiles for dry powder inhalers. Recently, the impactors have been shown to have manufacturing inconsistency and wear-induced changes in its stage cut points (Stein

and Olson, 1997; Marple et al., 1998). In addition, the impactor has also been criticized for wall losses and interstage leakage (Marple et al., 1998; Mitchell et al., 1998). Considering the questionable reliability of the impactor, verification of the impactor's accuracy is warranted.

To date, no published data is available which addresses the quantity and quality of dust generated when orthodontic adhesives are air-rotary abraded or whether traditional dental masks effectively filter the dust generated. This project determined the effectiveness of a series of masks to remove dust particles within the aerodynamically respirable size range, and attempted to characterize the size of the particles that are able to penetrate the mask. This project also determined whether the 8-stage impactor used to separate the different particle sizes does this accurately.

Materials and Methods:

Composite Sample Fabrication

Transbond XT (3M Unitek, Monrovia, CA), a commercially available light cured orthodontic resin composite adhesive was examined. The filler type in Transbond XT is quartz, with a weight percent of 70 and an average size of 3 μm, as reported by the manufacturer. A vacuum mold of a 3 mm thick x 12 mm diameter disk with a small projection ("handle") was made using 1.5 mm x 125 mm round Bioplast (Scheu-Dental, Iserlohn, Germany) material in a Ministar S (Great Lakes, Tonawanda, NY) machine. Twenty five composite disks were fabricated using the mold and cured for 60 seconds using an Ortholux LED curing light (3M Unitek, Monrovia, CA) with an irradiance of 1000 $mWcm^{-2}$, emitting light in the range of 430–480 nm (Fig. 1). They were weighed on a digital balance (A&D Company, Model GR-120, Tokyo, Japan) to a tenth of a milligram with the mass recorded as M_i. Three composite samples were ground into dust for each trial.

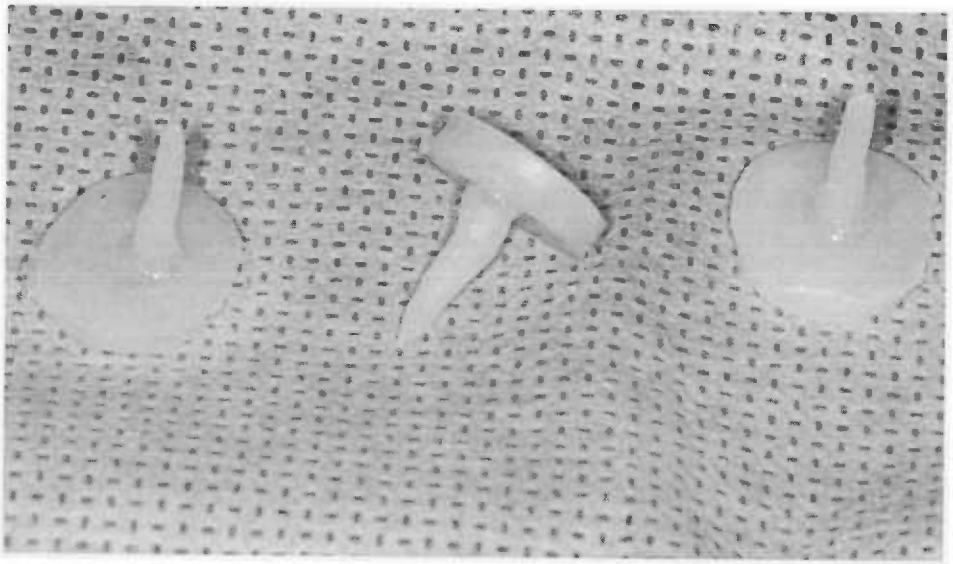

Figure 1. 3 Composite samples showing disk that was abraded and attached handle

Dust Collection

The testing apparatus used to collect the dust generated consisted of a 50 x 35 x 30 cm Plexiglas box connected to a multi-stage, multi-jet, Cascade Impactor type air-sampler (Tisch Environmental, Model 20-800, Cleves, OH) (see appendix A) with attached vacuum pump (Reliance Electric, Model 1531-107B-G557X, Gallipos, OH). The air-sampler was attached to a 2.54 cm hole in the wall of the box by way of a plastic hose. The vacuum pump, calibrated to draw 28.3 LPM, was attached to the air-sampler (Fig. 2.).

The collection apparatus was modified to include a mask placed over the intake orifice of the air sampler (Fig. 3 & 4). Separate trials using three different masks [1-Kimberly-Clark Tecnol Procedure Mask (Kimberly-Clark, Roswell, Georgia); 2-Kimberly-Clark Tecnol Cone Mask (Kimberly-Clark Worldwide, Inc., Roswell, Georgia); 3-3M Particulate Respirator N95(3M Occupational Health and Environmental Safety Division, model #8214, St. Paul, Minnesota)] were conducted (Fig. 5-7). In addition, three control trials, which were conducted without masks, were used for comparison. Two of these trials were performed in a previous study by Almeida (2006), while the third was performed in the current study. The same materials, methods and protocol were used for all trials.

The composite disks were ground into dust using a carbide finishing bur (7675, Brassler USA, Savannah, GA), in a high-speed handpiece (A-dec, Newberg, OR) without water spray. Light pressure and intermittent shaving strokes were used, which maintained a smooth, flat surface on the composite disk. The handpiece was run at 70 psi. During

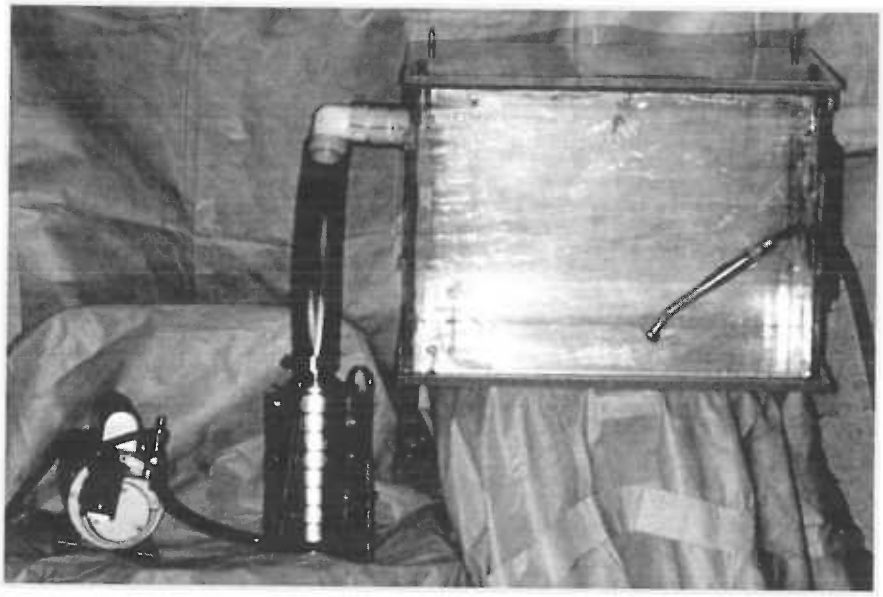

Figure 2. Test chamber with handpiece (R) with cascade impactor (center) attached to vacuum pump (L)

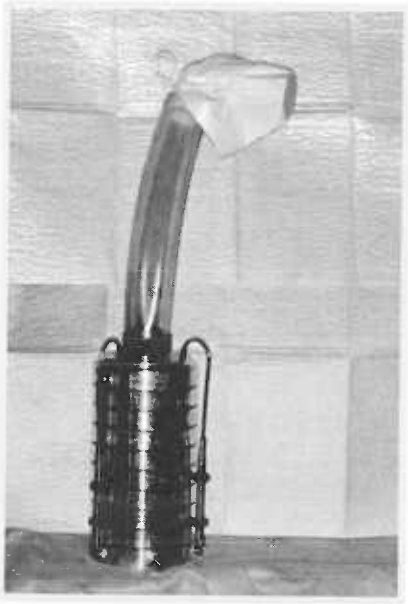

Figure 3. Impactor w/mask attached to intake

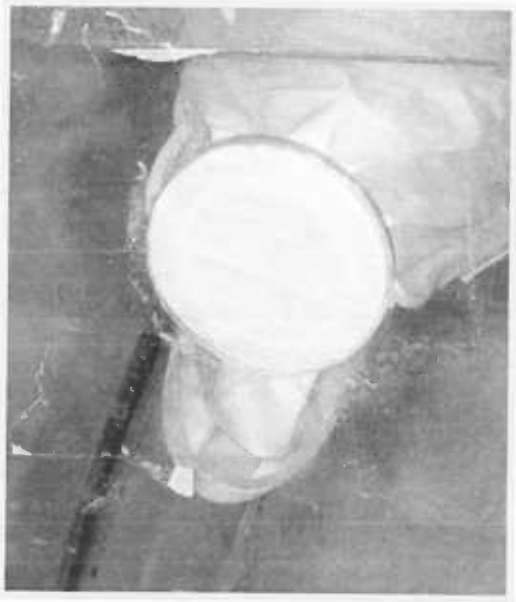

Figure 4. Mask viewed from inside collection chamber

grinding, aerosol from within the box was drawn into the air-sampler. The atmospheric pressure within the box was maintained by an open 2.54 cm diameter hole in the box opposite the intake assembly. The distance from the bur to the hole leading to the air-sampler was held at approximately 33 cm (13 inches). This has been cited as the average

distance an operator's head will be from the operating field (Chasteen, 1978). The vacuum pump remained on for 15 minutes after the disks were ground into dust while the chamber was aerated with a dental air/water syringe to free any trapped aerodynamically respirable dust. Following each run the collected dust was analyzed as described below and the apparatus was cleaned and reassembled with a new mask for the next sample to be processed. The bur was changed after grinding each disk.

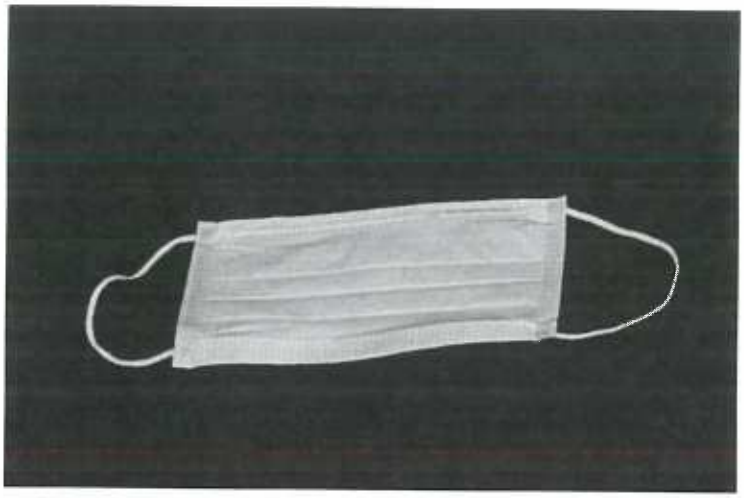

Figure 5. Kimberly-Clark Tecnol Procedure Mask (Kimberly-Clark, Roswell, Georgia)

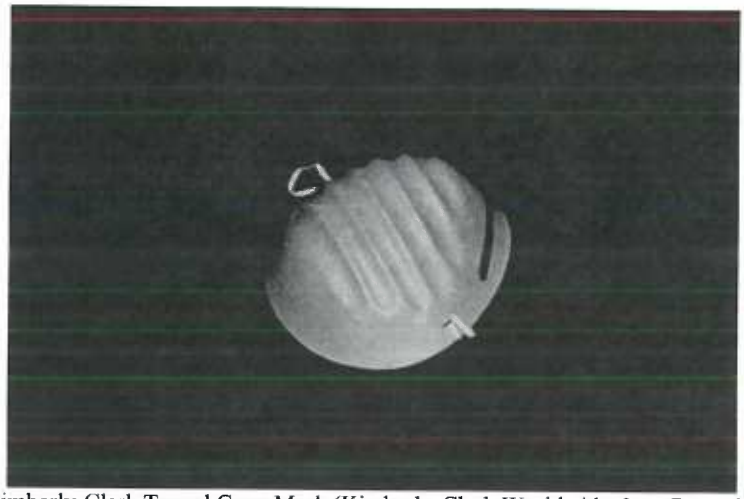

Figure 6. Kimberly-Clark Tecnol Cone Mask (Kimberly-Clark Worldwide, Inc., Roswell, Georgia)

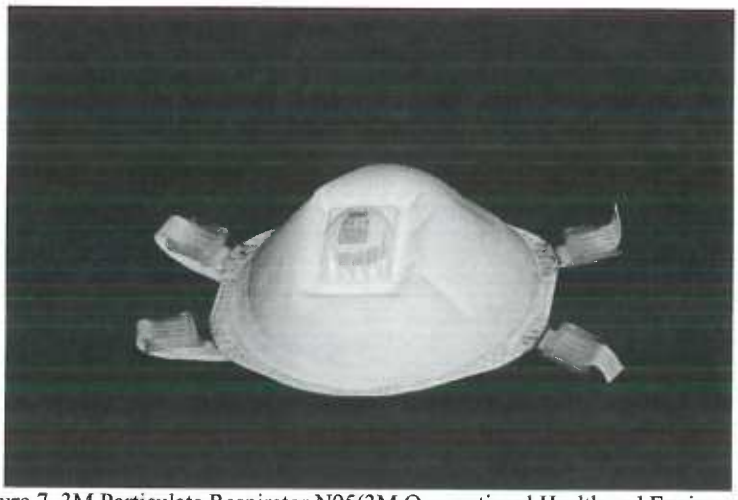

Figure 7. 3M Particulate Respirator N95(3M Occupational Health and Environmental Safety Division, model #8214, St. Paul, Minnesota)

Dust Segregation

Inside the air-sampler, dust particles were separated automatically into the eight stages of the compactor based on aerodynamic diameter (see appendix A) as shown in Figure 8. According to the manufacture's specifications, 95% of unit density spherical particles collected in each stage will be within the particle size cutoff values listed in Figure 9. This diagram also depicts where the fractions, if inhaled, would settle in the human respiratory tract.

According to the manufacturer, the mean and median diameters of particles collected in a stage were assumed to be equal, based on the assumption of a normal distribution (see Appendix A). This particle size was referred to as the mass median diameter (MMD). The MMD of unit density spheres (d_o) for each stage were calculated. The particle density (p_c) was normally estimated at 1.0 g/cm^3. The stage cut-off values were used to determine each particle's Equivalent Aerodynamic Diameter (AED). Based on the definition of aerodynamically respirable dust as having particles that range in size from 0.5-5.0 μm, any dust found on stages 3-8 was considered aerodynamically respirable.

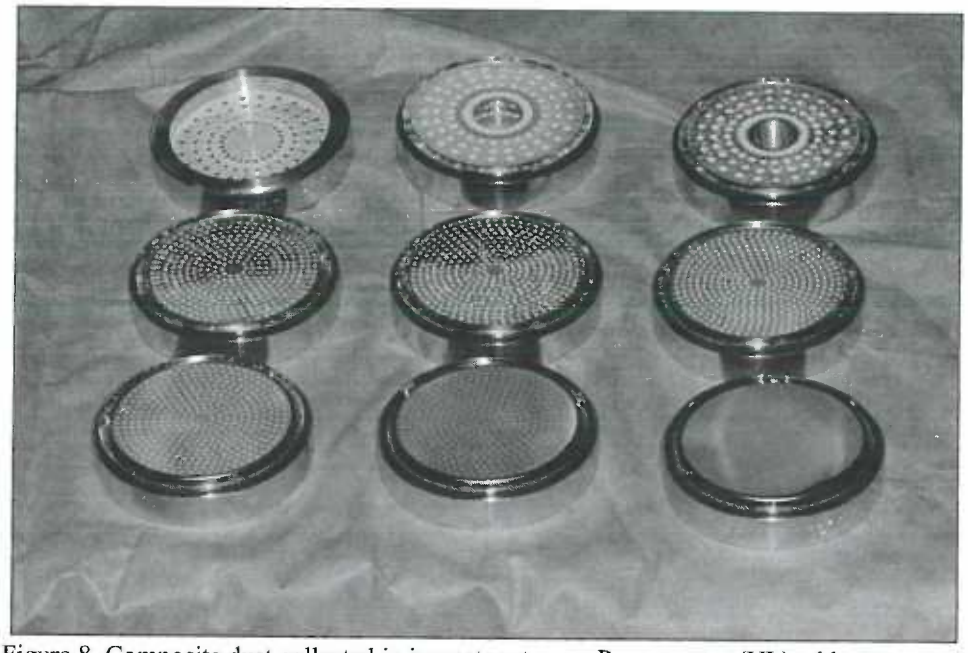

Figure 8. Composite dust collected in impactor stages. Preseparator (UL) with stages 1 through 8 (L to R and U to D)

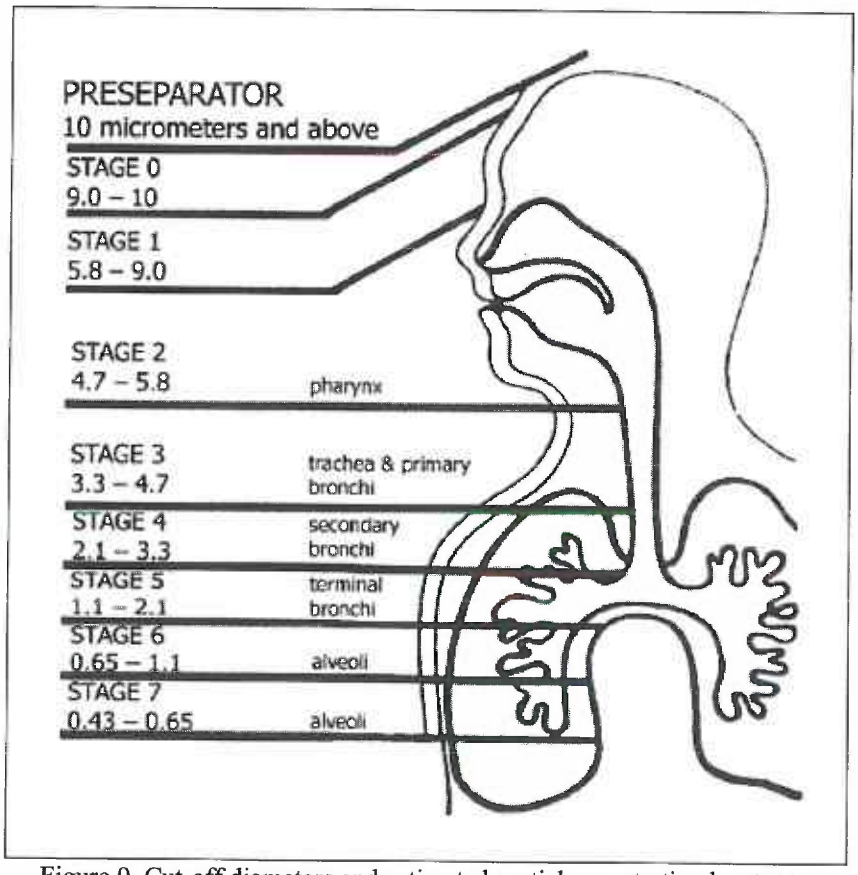

Figure 9. Cut-off diameters and estimated particle penetration by stage (modified from Tisch Cascade Impactor manual pg. 7)

Mass of Dust Collected

The mass of the collected dust was analyzed using the formula suggested by Collard et al. (1991) and the manual provided with the Cascade Impactor by Tisch Environmental. The composite handles were removed from the box, collectively weighed and the mass recorded as M_H. This value was subtracted from the initial mass (M_i) to determine the mass of dust generated (M_{DG}): $M_{DG} = M_i - M_H$. The air-sampler was disassembled, the eight trays removed and individually weighed, and the net mass of dust collected in each stage (MS_n; where n indicates the stage number, i.e. n=0,1,….,7) was determined by subtracting the weight of the tray alone which was measured prior to each experiment. The total mass of dust collected (M_{DC}) in the eight stages was determined by:

$$M_{DC} = \Sigma\, MS_n$$

The mass percent dust collected (MPDC) out of the total generated dust mass was determined by:

$$MPDC = (M_{DC}/M_{DG}) \times 100$$

The mass percent of dust collected in each stage was determined by:

$$(MS_n/M_{DC}) \times 100$$

Using Figure 9, the lower size was selected (smallest number) for each particle size range. This number represents the Effective Cut-Off Diameter (ECD) for each Impactor Stage. This ECD can also be determined by viewing Figure 10.

Stage #	Particle Diameter (microns)
0	≥ 9.0
1	5.8 - 9.0
2	4.7 - 5.8
3	3.3 - 4.7
4	2.1 - 3.3
5	1.1 - 2.1
6	0.7 - 1.1
7	0.4 - 0.7
8	0.0 - 0.4

Figure 10. Effective Cut-Off Diameter

The results of the particle size analysis was plotted as a Log-Probability graph with the Effective Cut-Off Diameter as the ordinate and the cumulative percent less than the particle size range by weight as the abscissa (Fig. 11). It has been commonly accepted that the Particulate Size Distribution should be presented in graphical form rather than reporting the Mass Mean Diameter and the Standard Geometric Deviation. By plotting the cumulative mass percent vs. the ECD, the particle concentration for any particle size range can be determined.

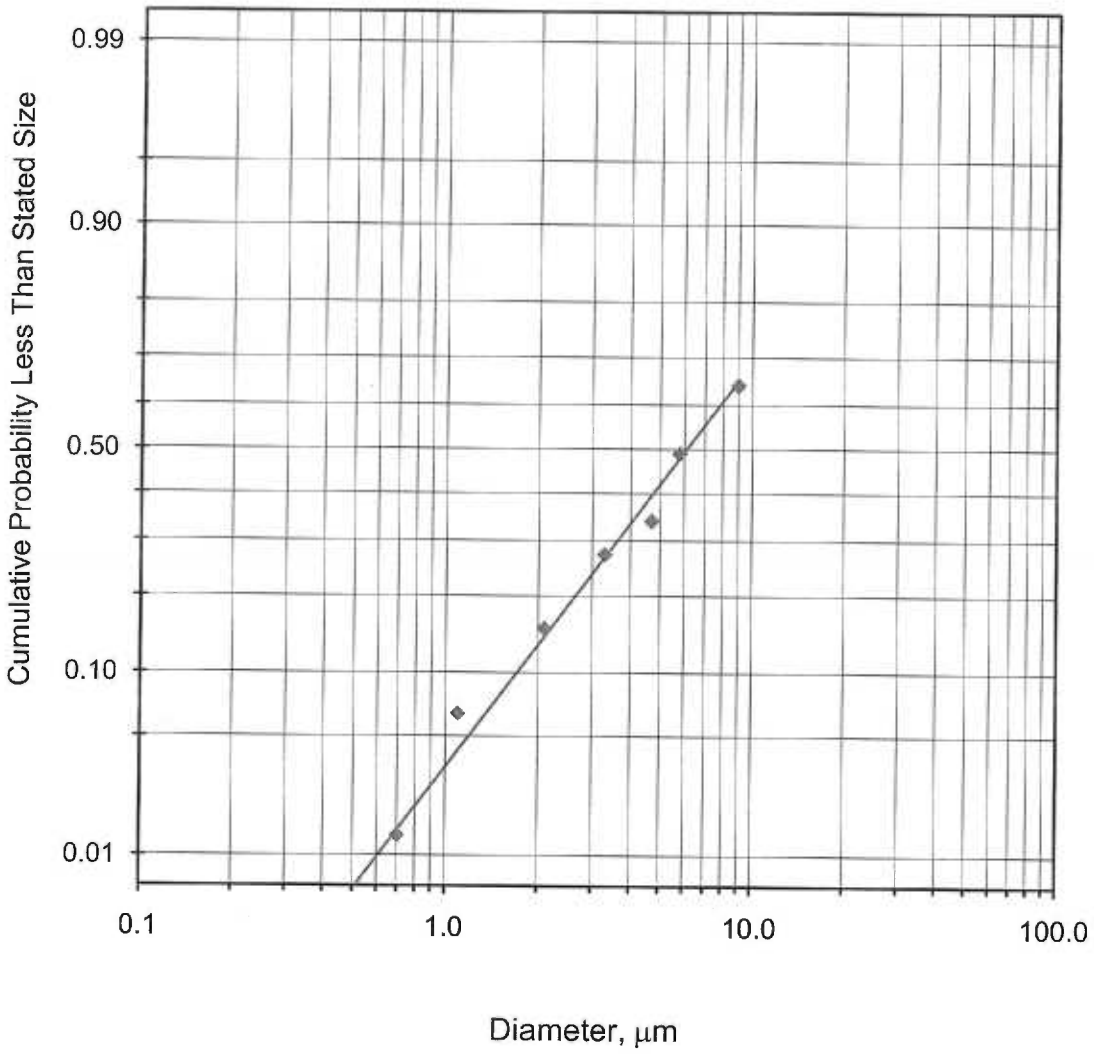

Fig. 11. Log probability graph of particle size vs. cumulative mass % less than stated size (Transbond Trial #1)

Estimated Number of Particles Collected

The estimated number of particles was determined using the method provided by Tisch Environmental's Cascade Impactor manual. The number of dust particles collected in each stage (NS_n) is calculated by:

$$NS_n = MS_n/MP_n$$

MS_n is the mass of dust collected in stage n. MP_n is the mass of a MMD dust particle collected in the same stage, calculated by:

$$MP_n = \rho_c \times VP_n$$

ρ_c is the particle density (measured as 2.0 g/cm^3 for the composite tested in this study, and 3.6 for the alumina polishing powders) and VP_n is the volume of a MMD dust particle collected in the same stage. For a spherically shaped MMD dust particle, $VP_n = (\pi/6 \times (d_c))^3$, where d_c is the diameter of the orifice jet for that particular stage. The total number of dust particles collected (N_{DC}) in the eight stages is determined by:

$$N_{DC} = \Sigma NS_n$$

The percent of the dust particles collected in each stage was determined by: $(NS_n/N_{DC}) \times 100$. The cumulative percent of dust particles collected for the stages below was plotted against d_c for each stage on a log-probability graph. Using ANOVA and Tukey's test ($p \leq 0.05$), the total mass collected and estimated number of particles for each type of dental mask were compared statistically to each other and to control trials involving no mask covering the opening to the impactor.

Accuracy of 8-Stage Impactor

To verify the accuracy of the 8-stage cascade impactor, aluminum oxide particles from three different polishing powders (Buehler Ltd., Evanston, IL) of differing sizes were aerosolized in the plexiglass box with the testing apparatus attached to collect the powders. Separate trials were performed for each particle size examined (0.3 μm, 1 μm, and 5 μm). These particles were then separated and weighed as before to determine the

efficacy of the impactor in separating the different particle sizes in the appropriate stages of the impactor. An attempt was made to prevent the particles from agglomerating together by aerating the powder in the plexiglass box with a fine stream of compressed air before the particles entered the impactor. The vacuum pump remained on for 10 minutes while the powder was aerated with the compressed air. Following each run the collected dust was analyzed as described above, and the apparatus was cleaned and reassembled for the next sample to be processed. The mass of the collected dust was analyzed as described earlier and was compared to the predicted result. Although the actual particle size distribution of the polishing powders was not known, it was assumed to be monomodal and relatively narrow based on the need for quality control in a commercial product designed for producing high quality polish. A second trial for each particle size examined was performed with a Kimberly-Clark Tecnol Procedure Mask covering the intake to further decrease the ability of the particles to agglomerate. The procedure mask was anticipated to help to break up or catch the particles that did agglomerate before reaching the mask.

In addition, four dust samples collected in the 8-stage impactor were analyzed with a Microtrac S3500 Series Particle Size Analyzer with Tri-laser Technology (Microtrac, Montgomeryville, PA). The Microtrac S3500 Particle Analyzer is based on Stokes-Einstein theory of light scattering. During the test, the particles were placed in solution using deionized water at 25°C and circulated through the detector cell. The density of the Transbond XT was determined ahead of time using Archimedes method of measuring the weight of a sample of cured Transbond XT in water and in air, with the resultant density of Transbond XT being 2.04 g/cm^3. The standard glass refractive index of 1.51 was used. While the monomer and filler in a composite typically have slightly

different refractive indices, they become closer during curing and are not likely to vary by more than 1-2% in the cured composite (Shortall et. al., 2008).

During a measurement cycle, three separate lasers are directed toward the sample at different angles of incidence and the resultant scattered light information from all three lasers was combined to generate particle size distributions. Four samples were analyzed with the Microtrac S3500. Sample #1 was a collection of the dust generated from grinding Transbond XT in which a Kimberly-Clark Tecnol Cone Mask was placed over the intake Samples #2-#4 were collections of dust generated from grinding Transbond XT with no mask over the intake. The samples were collected from the different stages as follows: Sample #2 included stage 1 (particle size range of 5.8-9 microns); Sample #3 included stages 2-3 (particle size range of 3.3-5.8 microns); Sample #4 included stages 4-7 (particle size range of .43-3.3 microns). The estimated number of particles was determined using the aforementioned method provided by Tisch Environmental's Cascade Impactor manual and compared to the results from the Microtrac S3500 particle analysis using two-way ANOVA and Tukey's test ($\alpha \leq 0.05$).

In an attempt to verify the results of the particle analysis, particles were collected from Trial # 2, in which the cone dental mask was used to filter particles generated from grinding the composite disks. The uncoated particles were separated according to stage and imaged using low voltage scanning electron microscopy (SEM)(Quanta 200, FEI, Hillsboro, Oregon). Stages 2 (4.7-5.8 μm), 5 (1.1-2.1 μm) and 7 (0.4-0.7 μm) were qualitatively compared to the predicted size range of the 8-stage impactor.

In addition, the procedure dental mask and the cone dental mask were viewed using SEM to qualitatively evaluate any differences in the design of the masks. The N95 mask was not viewed under SEM due to the difficulty in obtaining samples from the

mask after separating the multiple layers, which compromised the integrity of the mask. The procedure dental mask consisted of three separate layers which were inspected individually, while the cone dental mask was viewed from the top of the mask as well as a cross-section view of the mask.

Results:

Mask Comparison

Log Probability Graphs:

Log probability graphs for each transbond trial conducted were generated (Appendix B). The plots were generated by placing the Effective Cutoff Diameter as the ordinate and the cumulative percent less-than the stated particle size range by weight as the abscissa (see Fig. 11). This means a given point on the graph describes what percentage of the dust is equal to and smaller than the size stated. Log probability graphs are the standard means to display air sampling results, and allow for easy visualization of particle distribution. A first order linear regression plot has been included for each graph. This allows one to quickly reference where the particles of any given percentage are distributed and what particle size fraction it belongs to. For the trials with mask #3 (3M Particulate Respirator N95, no dust particles were collected in the 8-stage impactor and therefore log probability graphs were not generated.

Total Mass of Particles Collected / Mask:

The N95 mask trials displayed zero mass change in the impactor stages (Table I). Furthermore, no particles were noticed visually after the N95 mask trials. Therefore no further analysis of the N95 mask was deemed necessary.

Table I. Mass(in milligrams) of Transbond Collected with the N95 mask by Stage

	Impactor Stage							
Trial	1	2	3	4	5	6	7	8
1	0.00	0.00	0.00	0.00	0.00	0.00	0.00	0.00
2	0.00	0.00	0.00	0.00	0.00	0.00	0.00	0.00
AVG	0.00	0.00	0.00	0.00	0.00	0.00	0.00	0.00

For the remaining two mask categories examined (the Kimberly-Clark Tecnol Procedure Mask and the Kimberly-Clark Tecnol Cone Mask) and the control trials, statistical results of the total mass of composite particles collected in the impactor are shown in Appendix C, Table I. There was a statistically significant difference between the masks. Results of Tukey's test showed that the mass of particles collected in mask #1 (procedure dental mask) trials was significantly less than the mass of particles collected in mask #2 (cone dental mask) trials . When compared to a control (no mask over the intake), all of the mask trials collected significantly less particles by mass (Fig. 12;).

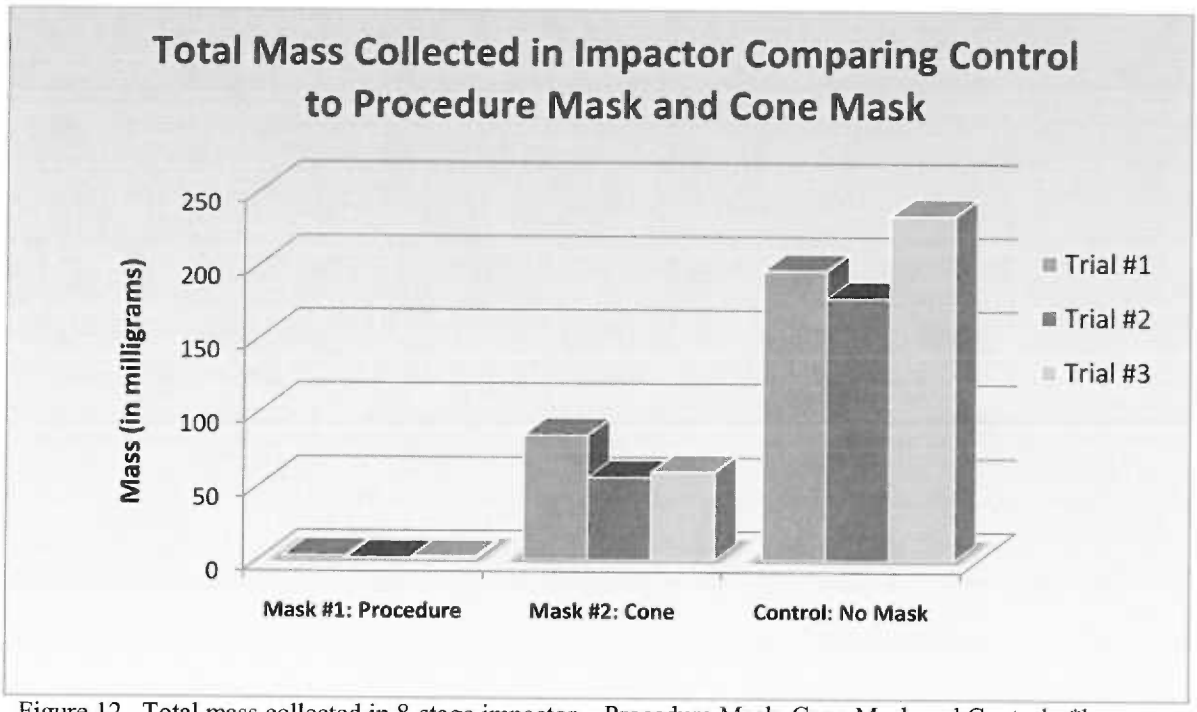

Figure 12. Total mass collected in 8-stage impactor – Procedure Mask, Cone Mask and Control. *horz. bars indicates sig. equivalent groups

Mass Percent of Total Particles Generated:

When evaluating the mass percent of composite that was collected in the impactor compared to the total mass of particles generated, similar results were shown (Fig. 13). Statistical results of the mass percent of particles collected in the Impactor are shown in

Appendix C, Table II. Without a mask covering the intake, 13% of the particles generated were collected in the impactor. The Procedure Mask allowed .03-.06% of the particles generated to pass, while the Cone Mask allowed 1-2.5% of the particles generated to pass. The procedure dental mask reduced the collected dust mass by over 99%, while the cone dental mask reduced the collected dust mass by 84% when compared to the control trials.

Results of the procedure mask and cone mask mass percents vs. stage number are shown in Appendix C, Table III. The mass percent of dust collected using the two masks distributed differently over the eight stages, however there was no difference between the mask types. This is because when the mass percentages are summed together by the statistical package each composite data set adds up to 100. For this reason there will be no difference when comparing these groups and the statistical software will report that the data sets are equivalent. There was a difference between the individual stages. Results of Tukey's test showed that the mass percent on each stage was statistically different for stages 1-3 and 5-6, while stages 4, 7 and 8 were statistically equivalent.

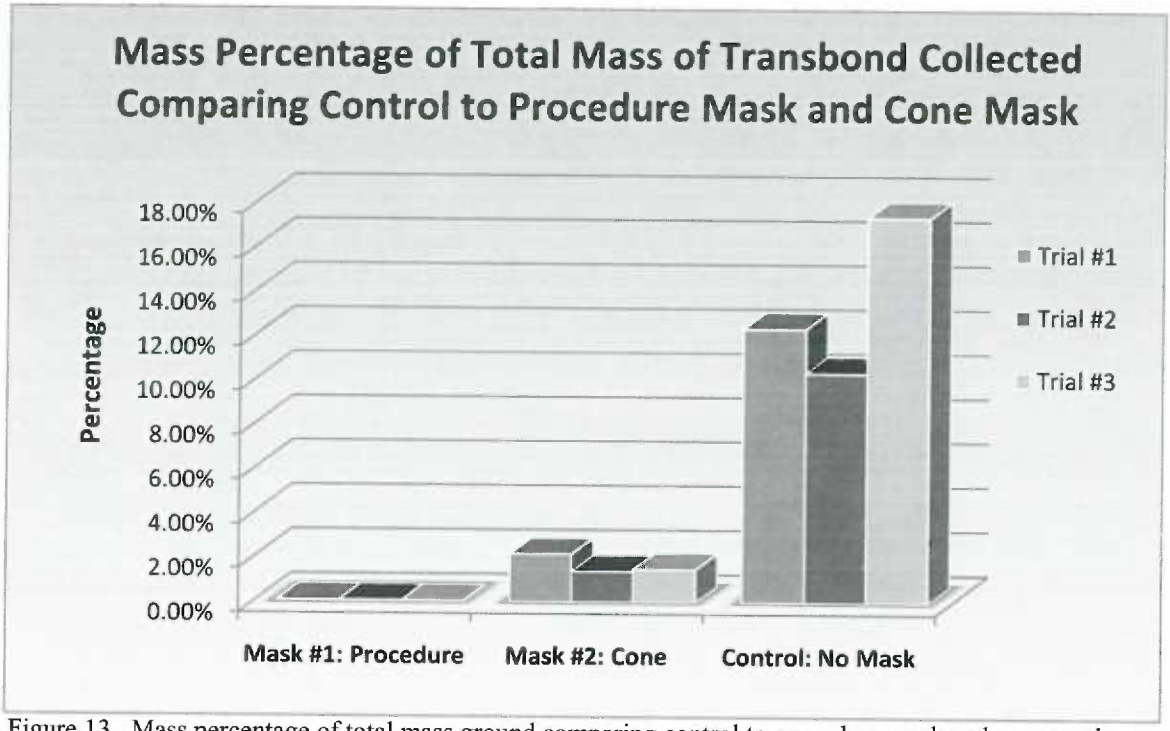

Figure 13. Mass percentage of total mass ground comparing control to procedure mask and cone mask
*horz. bars indicates sig. equivalent groups

Total Mass Collected / Stage:

Results of the total mass collected in each mask vs. stage number are shown in Appendix C, Table IV for the two dental masks examined (the Kimberly-Clark Tecnol Procedure Mask and theKimberly-Clark Tecnol Cone Mask). The total mass of dust collected from the composite adhesive distributed differently over the eight stages (Fig. 14), and there was a statistical difference between the mask types. Tukey's test showed that stages 1, 2, 3, 4 and 5 collected different masses when comparing the Procedure Mask to the Cone Mask. There was no statistical difference when comparing the mass collected from stages 6, 7 and 8.

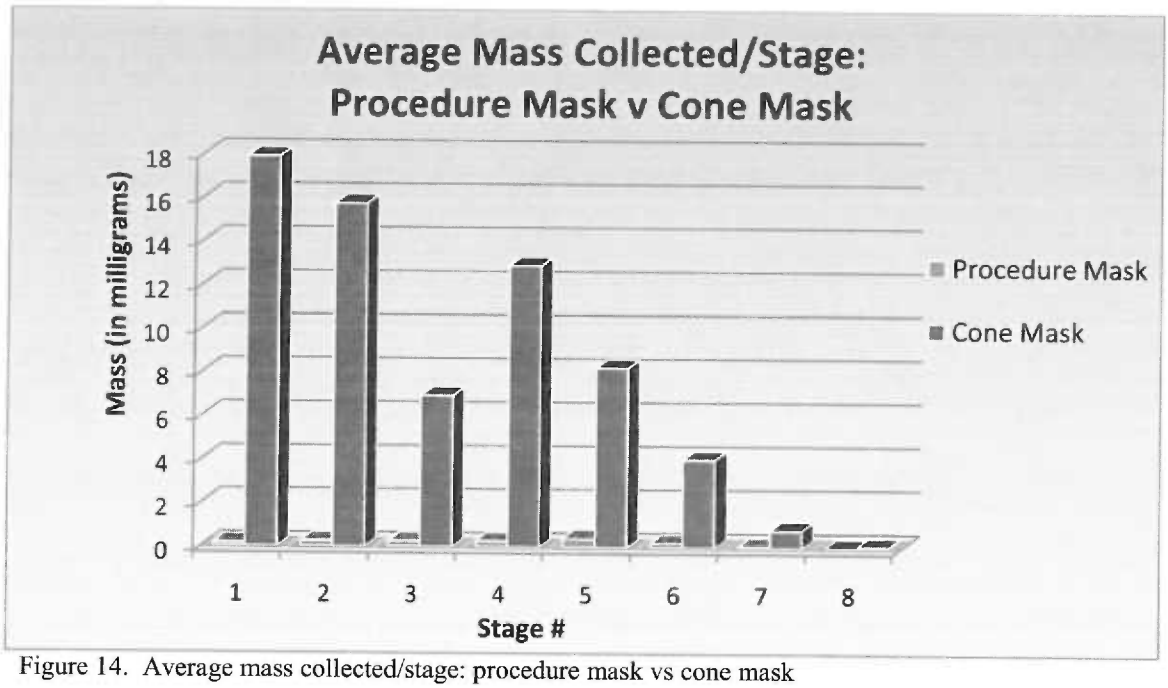

Figure 14. Average mass collected/stage: procedure mask vs cone mask

Estimated Number of Particles / Stage:

In the Procedure Mask sample, as particle size decreased, the number of particles found in each stage increased from stages 1-7, while stage 8 showed a lower particle count than stage 7 (Table II, Fig. 15). Approximately 6.95 x 10^7 particles were recovered from the aerodynamically respirable size range (stages 3-8).

Table II. Estimated Number of Particles of Transbond / Stage Collected with Procedure Mask

	Impactor Stage							
Trial	1	2	3	4	5	6	7	8
1	6.30E+04	1.55E+05	1.39E+06	2.92E+06	1.17E+07	2.66E+07	4.46E+07	0.00E+00
2	8.40E+04	1.03E+05	9.24E+05	1.95E+06	7.02E+06	3.54E+07	0.00E+00	0.00E+00
3	8.40E+04	1.55E+05	1.39E+06	2.92E+06	9.36E+06	1.77E+07	4.46E+07	0.00E+00
AVG	7.70E+04	1.38E+05	1.23E+06	2.60E+06	9.36E+06	2.66E+07	2.97E+07	0.00E+00
SD	1.21E+04	2.98E+04	2.67E+05	5.62E+05	2.34E+06	8.86E+06	2.57E+07	0.00E+00

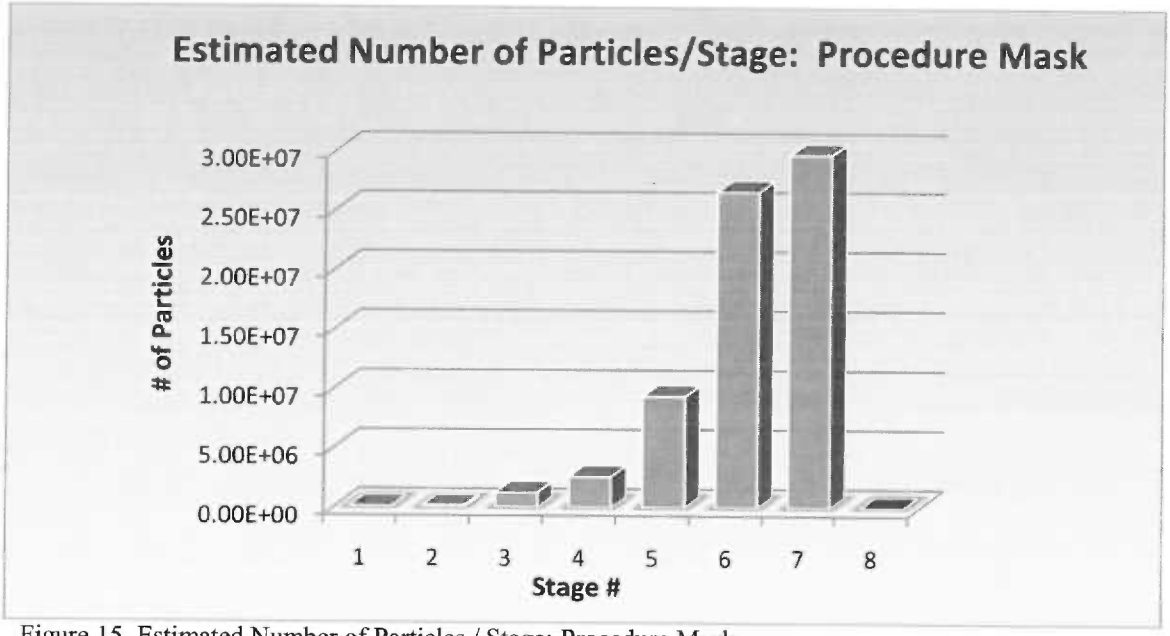

Figure 15. Estimated Number of Particles / Stage: Procedure Mask

The Cone Mask samples showed similar trends with increasing particle counts as the particle size range decreased for stages 1-6. Stages 7-8 showed a decrease in the number of particles when compared to those found in stage 6 (Table III, Fig. 16). Approximately 4.43 x 10^8 particles were recovered from the aerodynamically respirable size fractions (stages 3-8). Tukey's test showed that stages 4, 5, 6 and 7 collected statistically different number of particles when comparing the Procedure Mask to the Cone Mask. There was no statistical difference when comparing the number of particles collected from stages 1, 2, 3 and 8.

Table III. Estimated Number of Particles of Transbond / Stage Collected with Cone Mask

	Impactor Stage							
Trial	1	2	3	4	5	6	7	8
1	1.43E+06	3.46E+06	1.39E+07	5.26E+07	9.12E+07	2.04E+08	1.11E+08	2.23E+07
2	1.18E+06	2.73E+06	7.40E+06	4.18E+07	6.32E+07	1.33E+08	1.11E+08	2.23E+07
3	2.27E+06	5.06E+06	2.13E+07	7.98E+07	1.24E+08	1.86E+08	4.46E+07	0.00E+00
AVG	1.62E+06	3.75E+06	1.42E+07	5.81E+07	9.28E+07	1.74E+08	8.92E+07	1.49E+07
SD	5.72E+05	1.19E+06	6.94E+06	1.96E+07	3.04E+07	3.69E+07	3.86E+07	1.29E+07

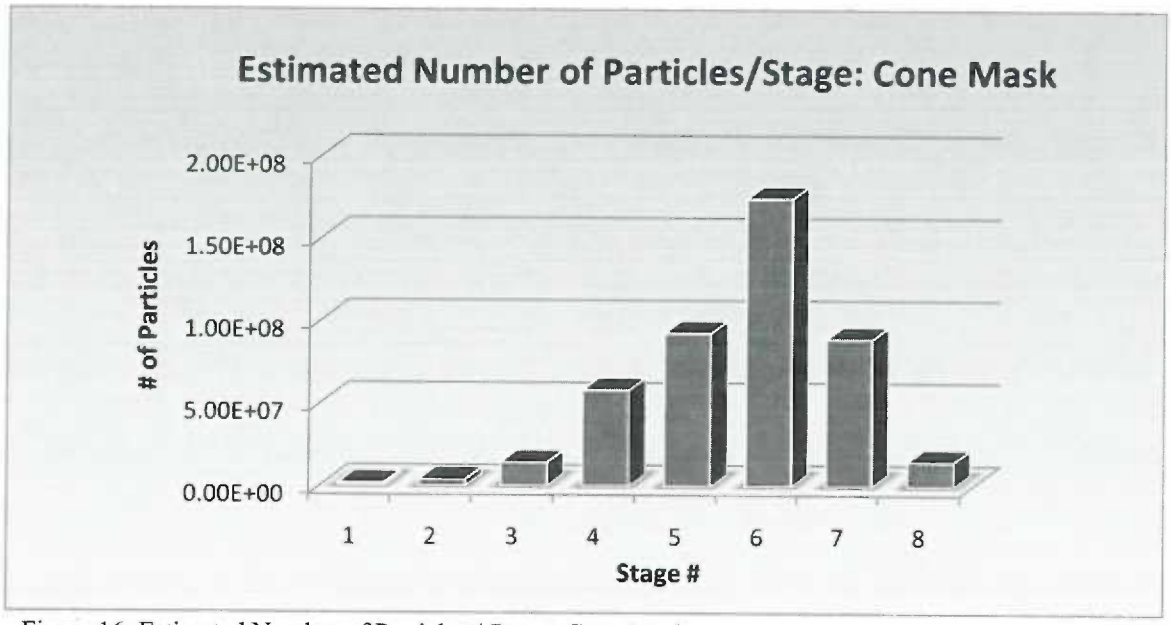

Figure 16. Estimated Number of Particles / Stage: Cone Mask

The control trials showed increasing particle counts as the particle size range decreased for stages 1-6, while stage 7-8 showed a lower particle count than stage 6 (Table IV). Approximately 6.54 x 10^9 particles were recovered from the aerodynamically respirable size range (stage 3-8).

Table IV. Estimated Number of Particles of Transbond / Stage Collected with no Mask

	Impactor Stage							
Trial	1	2	3	4	5	6	7	8
1	5.49E+07	8.85E+07	4.74E+08	9.60E+08	1.43E+09	2.39E+09	9.36E+08	4.68E+08
2	3.63E+07	6.21E+07	3.66E+08	8.01E+08	1.19E+09	2.00E+09	9.36E+08	2.01E+08
3	3.54E+07	7.83E+07	3.54E+08	8.91E+08	1.38E+09	2.90E+09	1.47E+09	4.68E+08
AVG	4.22E+07	7.63E+07	3.98E+08	8.84E+08	1.34E+09	2.43E+09	1.11E+09	3.79E+08
SD	1.10E+07	1.33E+07	6.61E+07	7.97E+07	1.25E+08	4.53E+08	3.08E+08	1.54E+08

Two-way ANOVA comparing the estimated number of particles passing through the cone-shaped dental mask and the estimated number of particles passing through the ear-loop dental mask with the estimated number of particles without using a mask

(control) was conducted and the results are shown in Appendix C, Table V. There was a statistically significant difference when comparing the two dental masks. When comparing the number of particles collected for the two dental mask trials, the cone mask allowed a significantly higher number of particles to pass through the mask than the procedure mask (Appendix D, Fig. 1). When comparing both the procedure mask and the cone mask to the control, there was also a statistically significant difference (Figure 17). The cone mask allowed 93.0% fewer aerodynamically respirable particles to pass through, while the procedure mask allowed 98.9% fewer aerodynamically respirable particles to pass through when compared to the control.

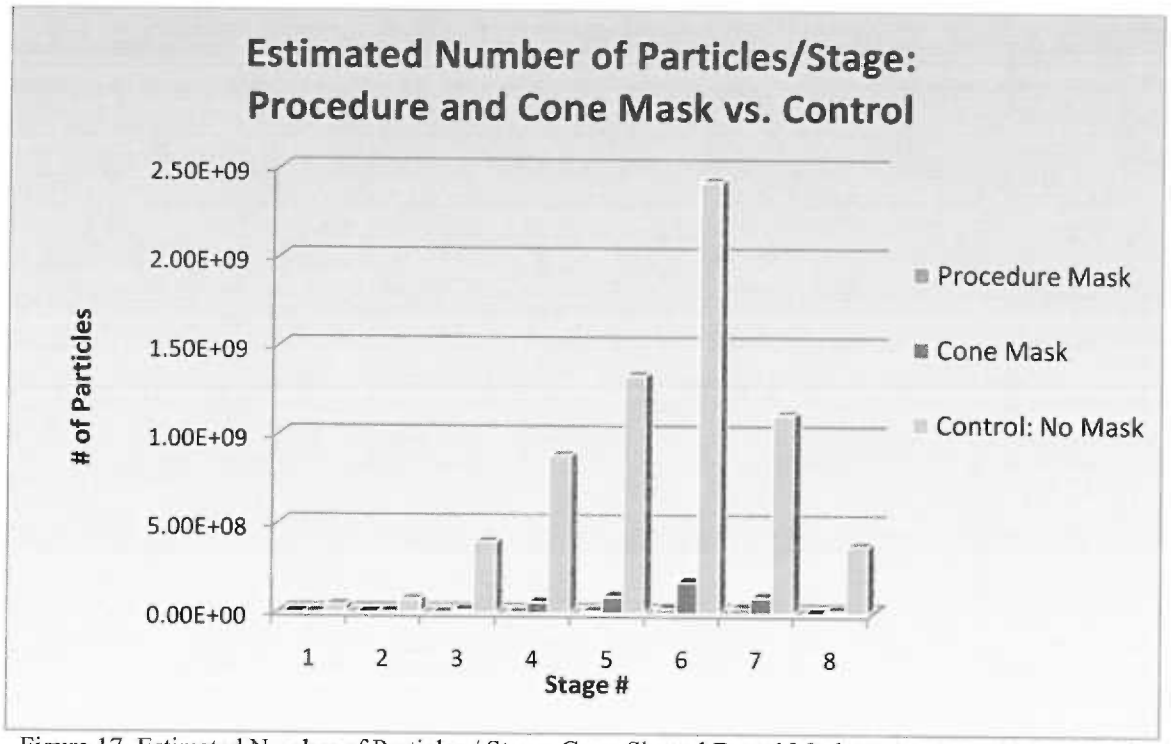

Figure 17. Estimated Number of Particles / Stage: Cone-Shaped Dental Mask vs. Ear-Loop Dental Mask vs. Control.

Accuracy of 8-Stage Impactor

Mass Percent Aluminum Oxide Particles / Stage

The mass percent of the aluminum oxide particles collected in the impactor is shown in Table V, Figure 18. For the 0.3 μm particles, 2.8% by mass was collected in stages 8, correlating to particles less than 0.43 μm. For the 1 μm particles, 11.4% by mass was collected in stages 6-8, which correlates to particles less than 1.1 μm. For the 5 μm particles, 68.4% by mass was collected in stages 2-8, which correlates to particles smaller than 5.8 μm. Percentages were calculated using the particles equal to or less than the anticipated particle size. When the polishing powder is made, the critical aspect is that the particles not be larger than the stated size, but smaller particles wouldn't compromise the quality control of the polishing powder. For this reason, the percentages were based on particles equal to or less than the stated size of the powder.

Table V. Mass Percent / Stage

Stage	Particle Size	0.3 micron	1 micron	5 micron
1	5.8-9	42.48%	40.95%	31.64%
2	4.7-5.8	16.78%	20.48%	31.85%
3	3.3-4.7	5.42%	6.67%	12.45%
4	2.1-3.3	9.09%	10.00%	12.28%
5	1.1-2.1	7.87%	10.48%	6.20%
6	.65-1.1	9.27%	9.52%	3.91%
7	.43-.65	6.29%	1.43%	1.29%
8	<.43	2.80%	0.48%	0.38%

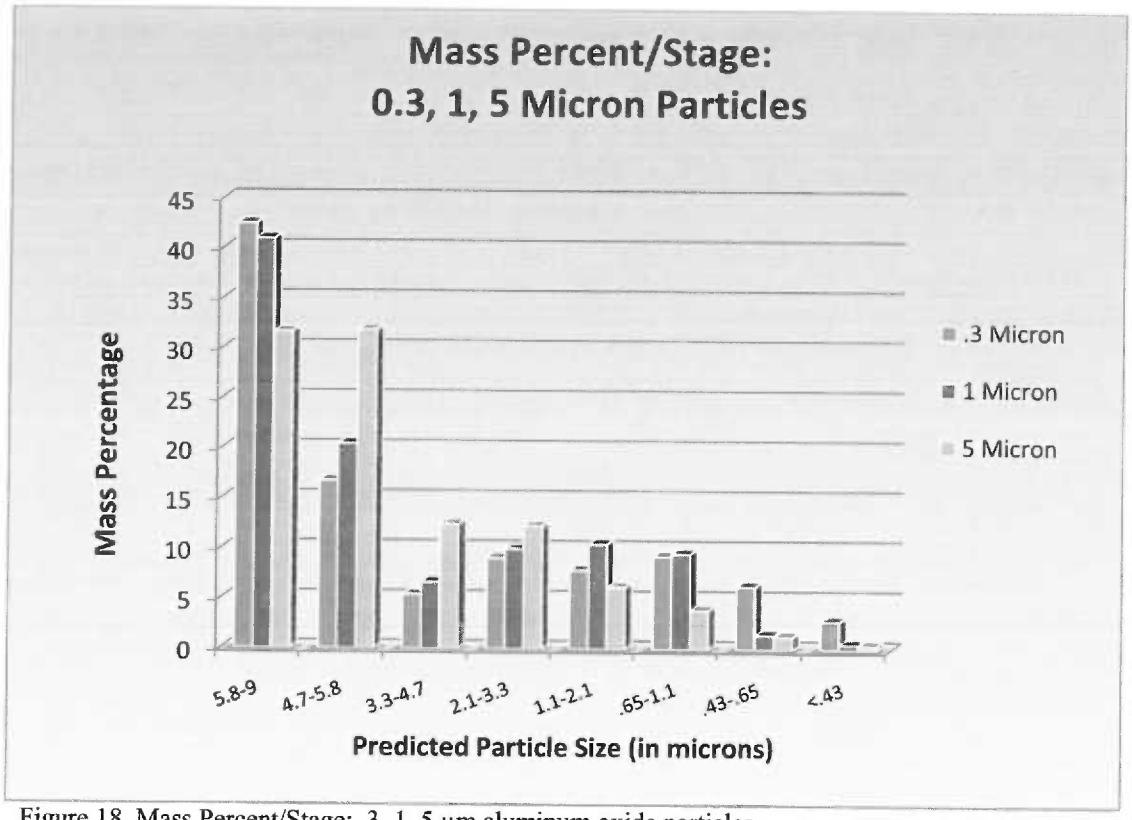

Figure 18. Mass Percent/Stage: .3, 1, 5 μm aluminum oxide particles

The mass percent of the aluminum oxide particles collected in the impactor with a procedure mask over the intake is shown in Table VI, Figure 19. For the 0.3 μm particles, 18.8% by mass was collected in stage 8, 25.1% of the 1 μm particles by mass was collected in stage 6, with an additional 4.7% correlating to particles smaller than 1 μm. For the 5 μm particles, 29.3% by mass was collected in stage 2, with an additional 45.3% correlating to particles smaller than 5 μm.

Table VI. Mass Percent / Stage(w/ mask over intake)

Stage	Particle Size	0.3 Micron	1 Micron	5 Micron
1	5.8-9	0.00%	22.51%	24.96%
2	4.7-5.8	0.00%	13.09%	29.31%
3	3.3-4.7	0.00%	4.71%	11.11%
4	2.1-3.3	25.00%	13.09%	20.13%
5	1.1-2.1	25.00%	16.75%	9.18%
6	.65-1.1	12.50%	25.13%	3.86%
7	.43-.65	18.75%	4.71%	1.13%
8	<.43	18.75%	0.00%	0.32%

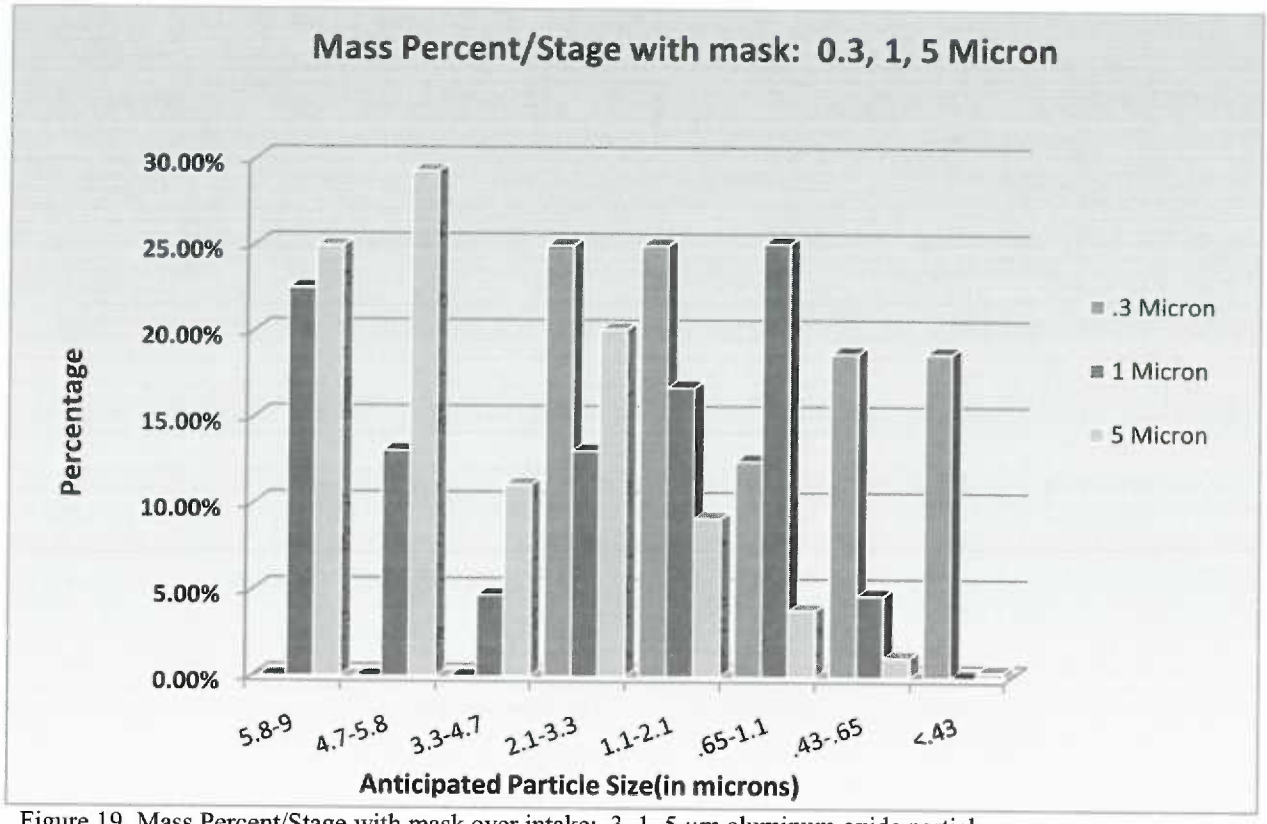

Figure 19. Mass Percent/Stage with mask over intake: .3, 1, 5 µm aluminum oxide particles

Estimated Number of Particles / Stage:

The mass percent was not an indicator of the number of particles represented in each stage. The estimated number of aluminum oxide particles collected in the impactor is shown in Table VII, Figure 20. For the 0.3 µm particles, 19.7% of the particles were collected in stage 8, correlating to any particles less than or equal to 0.43 µm. For the 1 µm particles, 76.4% of the particles were collected in stages 6-8, correlating to particles less than 1.1 µm. For the 5 µm particles, 99.4% of the particles were collected in stages 2-8, correlating to particles less than 5.8 µm.

Table VII. Estimated Number of Particles / Stage

Stage	Particle Size	0.3 micron	1 micron	5 micron
1	5.8-9	2.84E+06	1.00E+06	2.75E+07
2	4.7-5.8	2.75E+06	1.23E+06	6.79E+07
3	3.3-4.7	7.96E+06	3.60E+06	2.38E+08
4	2.1-3.3	2.81E+07	1.14E+07	4.94E+08
5	1.1-2.1	5.85E+07	2.86E+07	5.99E+08
6	.65-1.1	2.61E+08	9.85E+07	1.43E+09
7	.43-.65	4.46E+08	3.72E+07	1.19E+09
8	<.43	1.98E+08	1.24E+07	3.47E+08

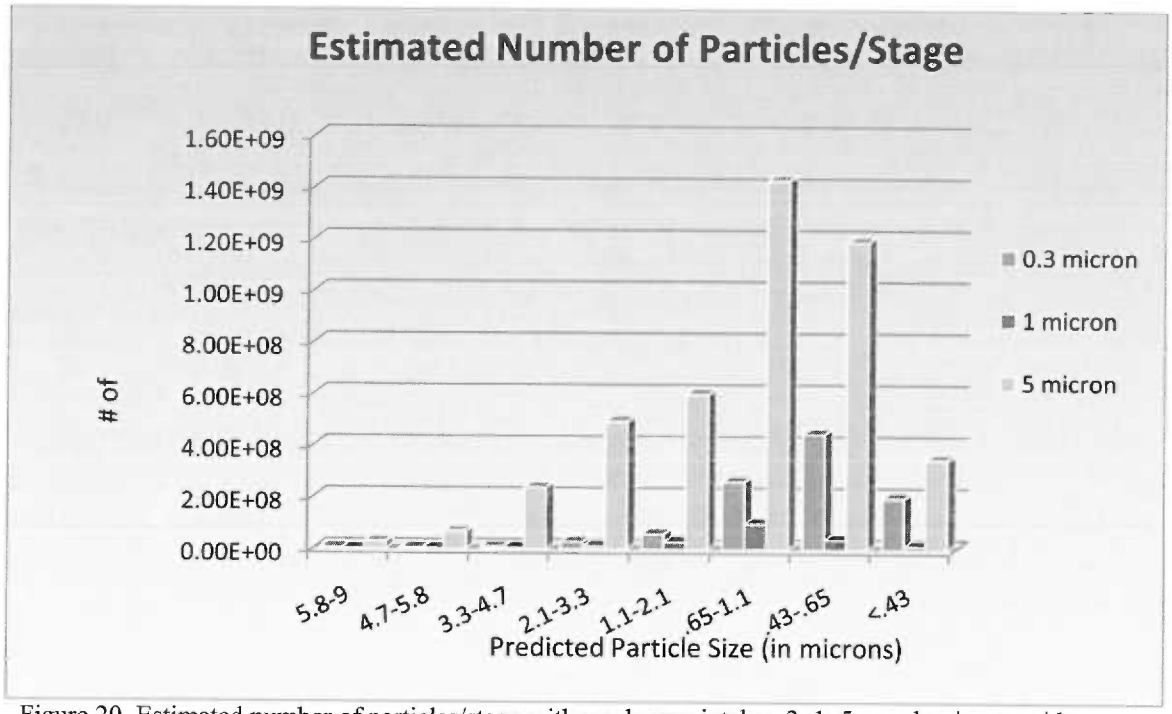

Figure 20. Estimated number of particles/stage with mask over intake: .3, 1, 5 μm aluminum oxide particles

The estimated number of aluminum oxide particles collected in the impactor with a procedure mask over the intake is shown in Table VIII, Figure 21. For the 0.3 μm particles, 40.6% of the particles were collected in stage 8, 85.6% of the 1 μm particles were collected in stages 6-8, while 99.5% of 5 μm particles were found in stages 2-8.

Table VIII. Estimated Number of Particles / Stage(w/ mask over intake)

Stage	Particle Size	0.3 Micron	1 Micron	5 Micron
1	5.8-9	0.00E+00	5.02E+05	1.81E+06
2	4.7-5.8	0.00E+00	7.17E+05	5.22E+06
3	3.3-4.7	0.00E+00	2.31E+06	1.77E+07
4	2.1-3.3	2.16E+06	1.35E+07	6.76E+07
5	1.1-2.1	5.20E+06	4.16E+07	7.41E+07
6	.65-1.1	9.85E+06	2.36E+08	1.18E+08
7	.43-.65	3.72E+07	1.11E+08	8.67E+07
8	<.43	3.72E+07	0.00E+00	2.48E+07

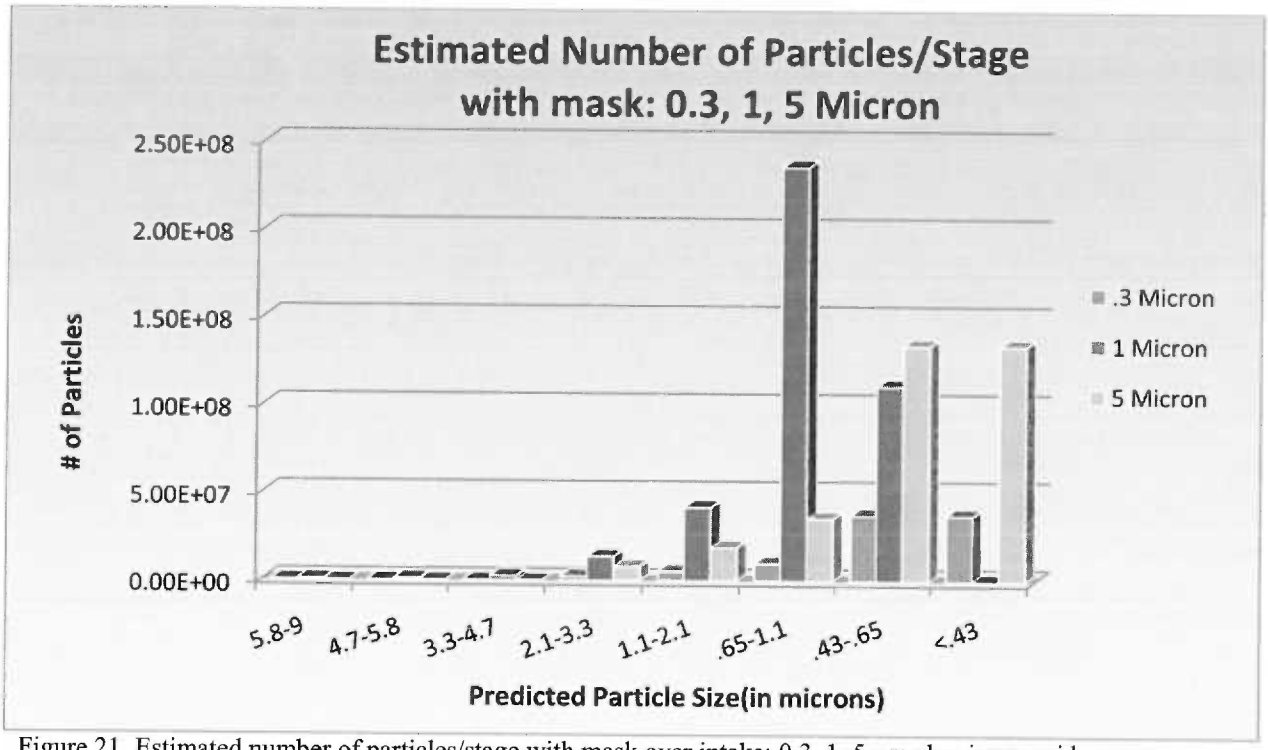

Figure 21. Estimated number of particles/stage with mask over intake: 0.3, 1, 5 μm aluminum oxide particles

Microtrac S3500 Series Particle Size Analyzer

Log probability graphs for each sample analyzed are shown in Appendix D. The first sample analyzed included the particles collected in the 8-stage impactor without a mask over the intake. The estimated number of particles collected from the 8-stage impactor is shown in Figure 22 as a percentage of the total number of particles collected,

along with the percentages in each size range as determined by the Microtrac S3500 particle analyzer. According to the Microtrac S3500 particle analyzer, approximately 95% of the particles were less than or equal to 1.1 μm, while the 8-stage impactor shows that approximately 46% of the particles were less than or equal to 1.1 μm.

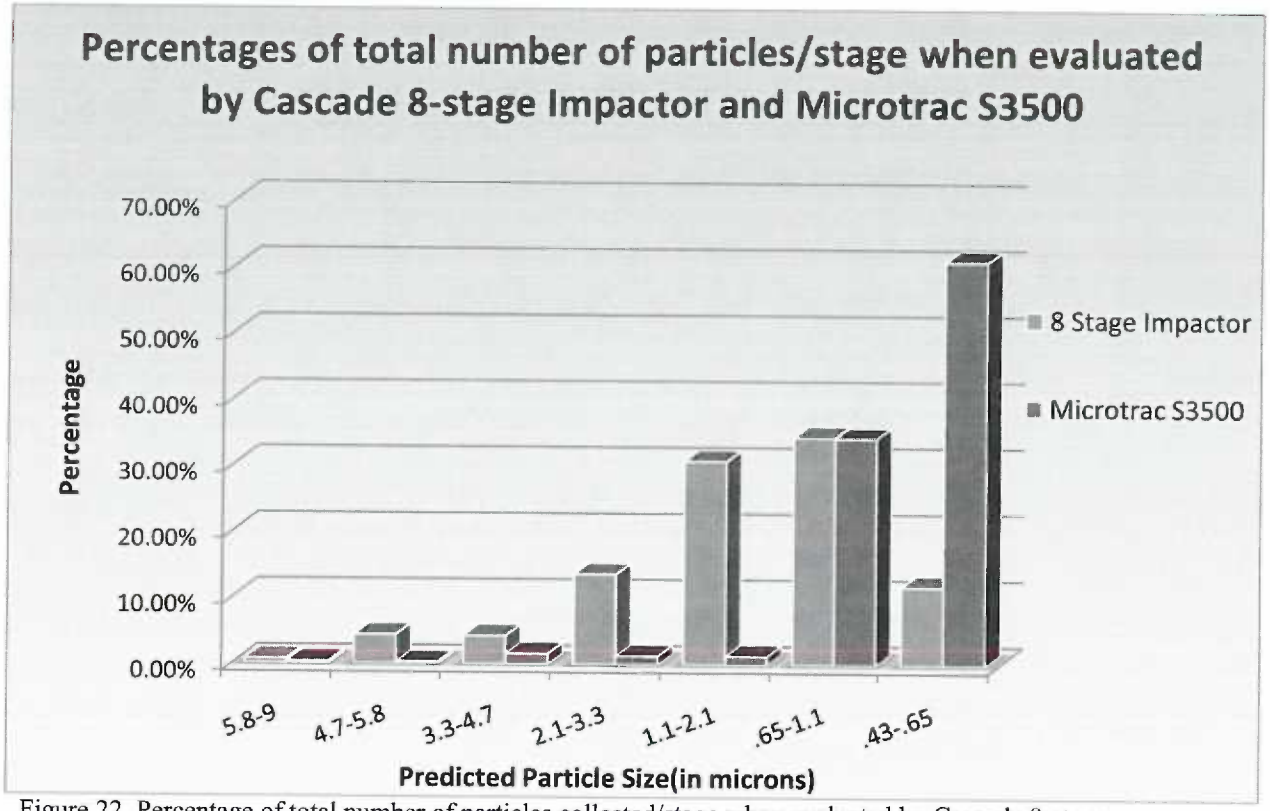

Figure 22. Percentage of total number of particles collected/stage when evaluated by Cascade 8-stage impactor and Microtrac S3500

For samples #2-4, the estimated number of particles expressed as a percentage are shown in Table IX. According to the Microtrac S3500, 0.08% of the particles analyzed from sample #2, which consisted of stage #1 particles, were in the appropriate size range of 5.8-9 μm. For sample #3 (stages 2-3), 0.73% of the particles analyzed were in the appropriate size range, while 43.6% of the particles in sample #4 (stages 4-7) were in the appropriate size range.

Table IX. Percentage: Number of Particles / Sample

		Percentage of Particles in Particle Size Range		
SAMPLE	Stage #	8-Stage Impactor	Microtrac S3500	Particle Size Range
#2	1	100.00%	0.08%	5.8-9.0
#3	2	54.54%	0.17%	4.7-5.8
	3	45.46%	0.56%	3.3-4.7
#4	4	14.03%	2.24%	2.1-3.3
	5	32.27%	3.16%	1.1-2.1
	6	46.21%	30.71%	.65-1.1
	7	7.49%	63.89%	.43-.65

Scanning Electron Microscopy

The particles from stages 2, 5 and 7, which were examined with scanning electron microscopy, are shown in Figures 23, 24 and 25 respectively. If the 8-stage impactor accurately separated the particles according to size range, the particles in stage 2 would be between 4.7 and 5.8 μm. However, particles can be found ranging from less than 1 micron to 10 μm. Particles from stage 5, which correlates to particles in the 1.1-2.1 μm size range, were more difficult to visualize individually due to the particles being clustered together. However, particles from this stage can be found ranging from less than 1 μm to greater than 5 μm. The particles from stage 7 correlated much closer to the anticipated particle size of 0.43-0.65 μm, with particles ranging from 0.5-1 μm.

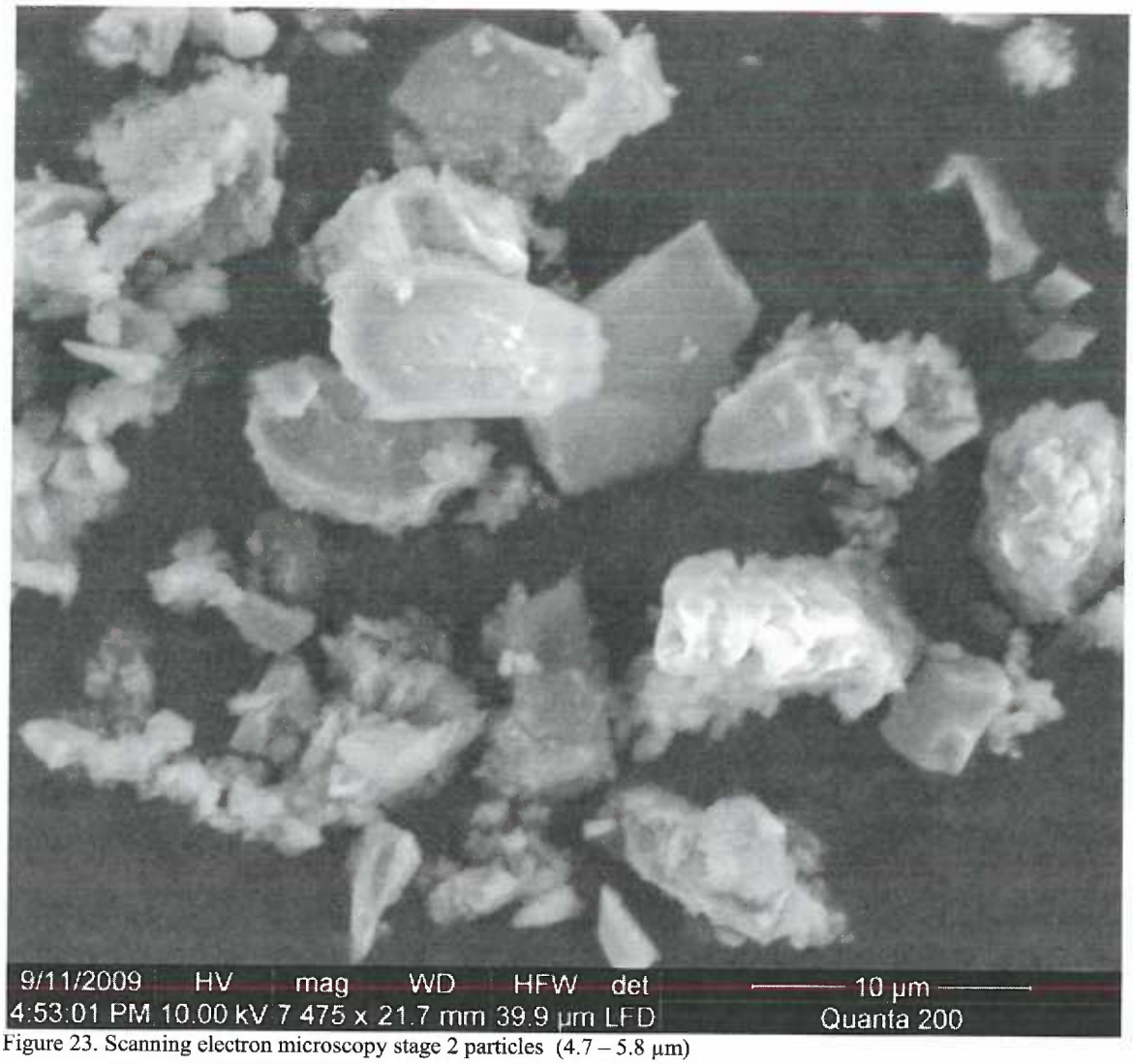

Figure 23. Scanning electron microscopy stage 2 particles (4.7 – 5.8 µm)

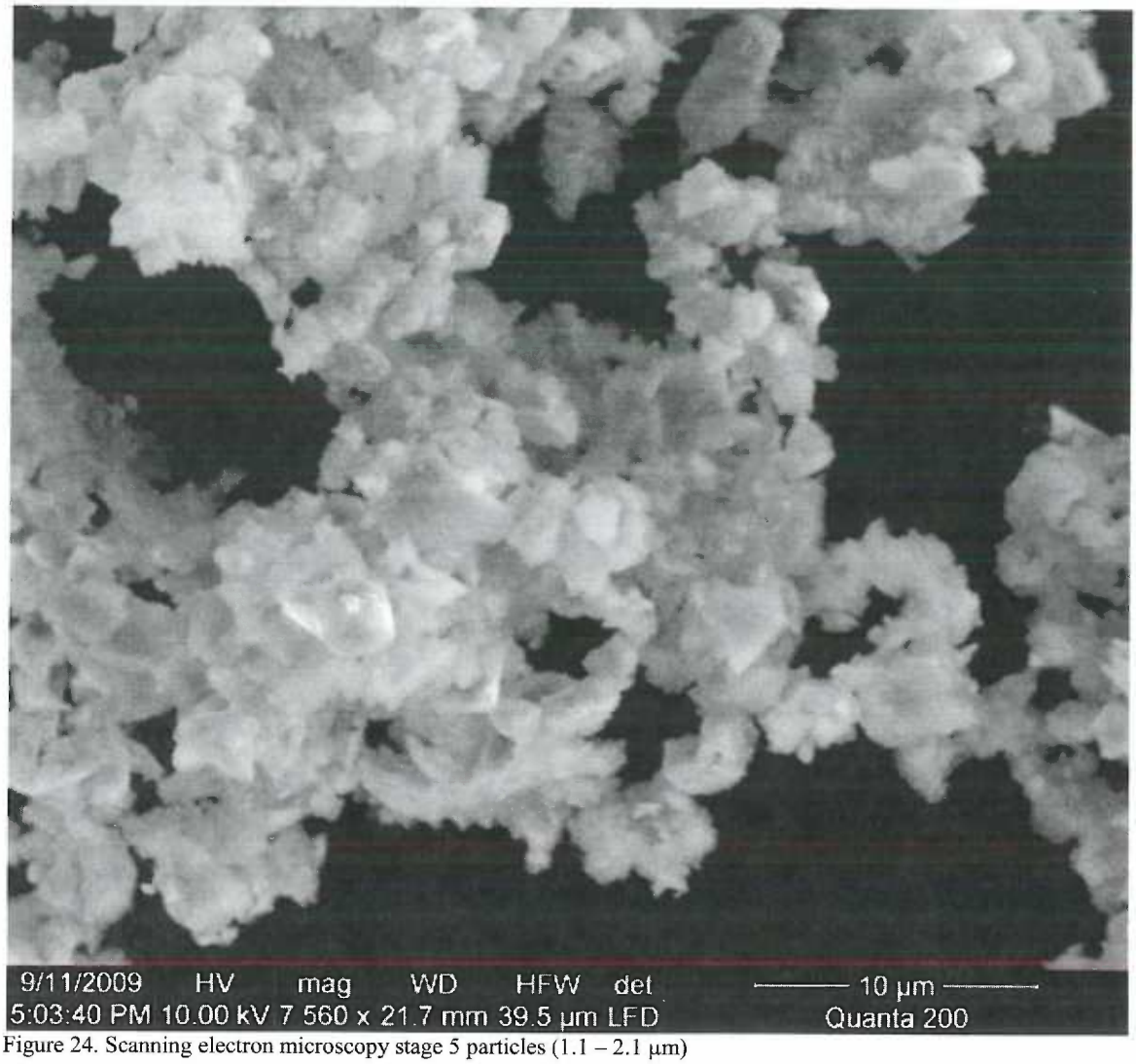

Figure 24. Scanning electron microscopy stage 5 particles (1.1 – 2.1 µm)

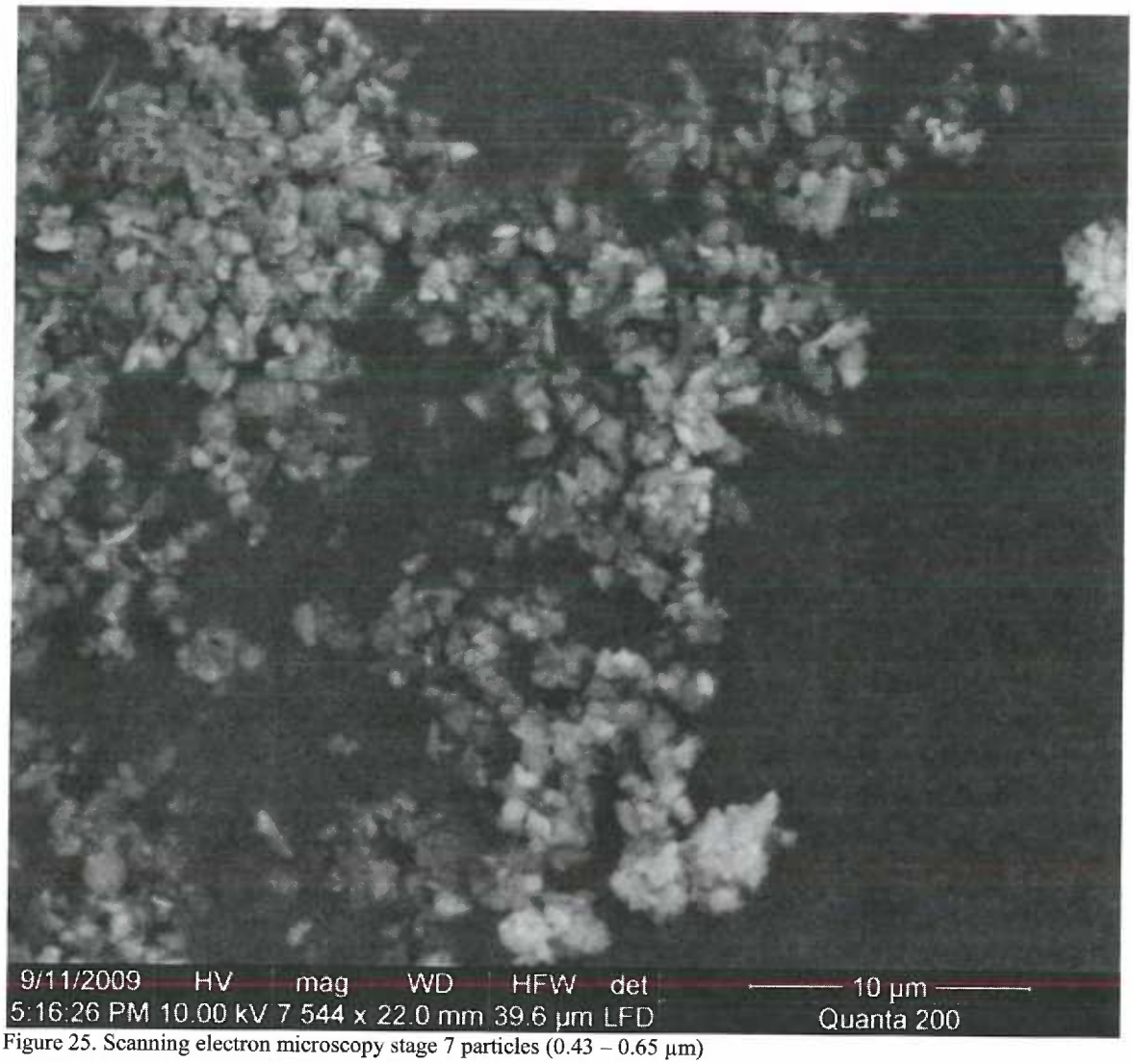

Figure 25. Scanning electron microscopy stage 7 particles (0.43 – 0.65 µm)

The two dental masks were examined with scanning electron microscopy. Figures 26-28 show the three layers of the procedure dental mask, while Figures 29-30 show the views of the cone dental mask. The fibers of the outer layers of the procedure mask appear flatter than the fibers in the cone dental mask, however the dental cone mask appears to have more fibers.

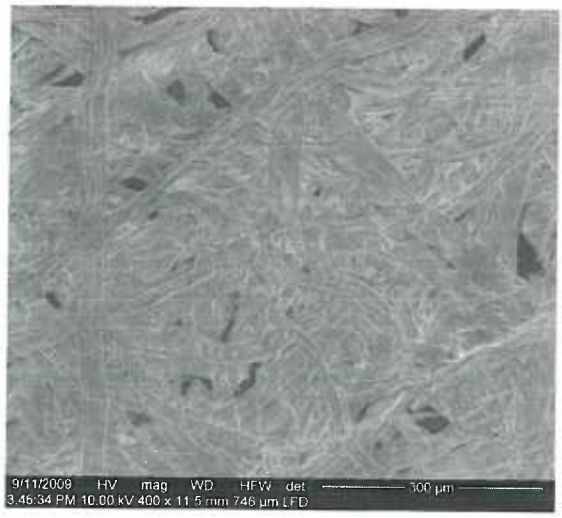

Figure 26. Scanning electron microscopy exterior of cone dental mask

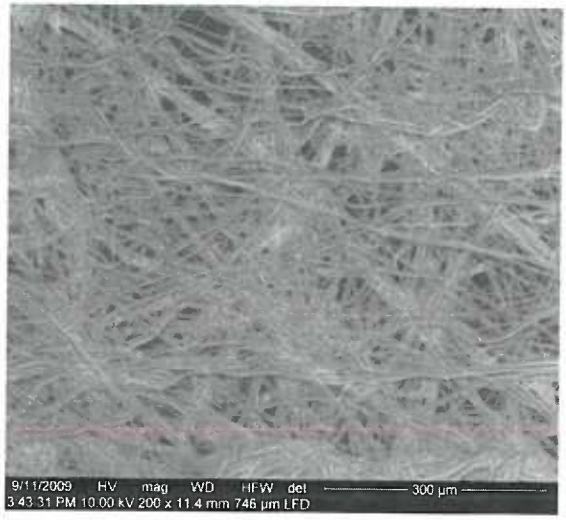

Figure 27. Scanning electron microscopy interior layer of procedure dental mask

Figure 28. Scanning electron microscopy exterior layer of procedure dental mask

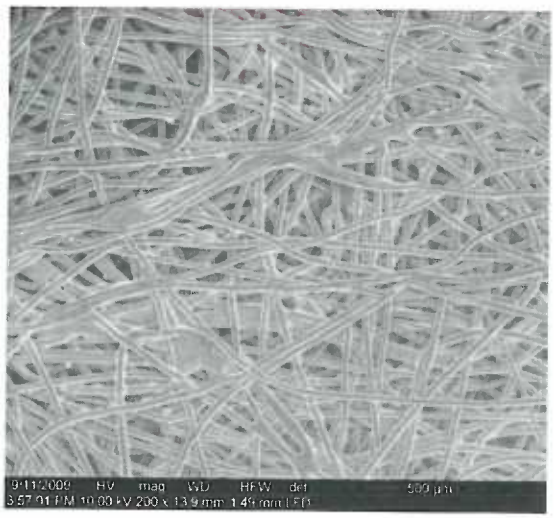

Figure 29. Scanning electron microscopy frontal view layer of procedure dental mask

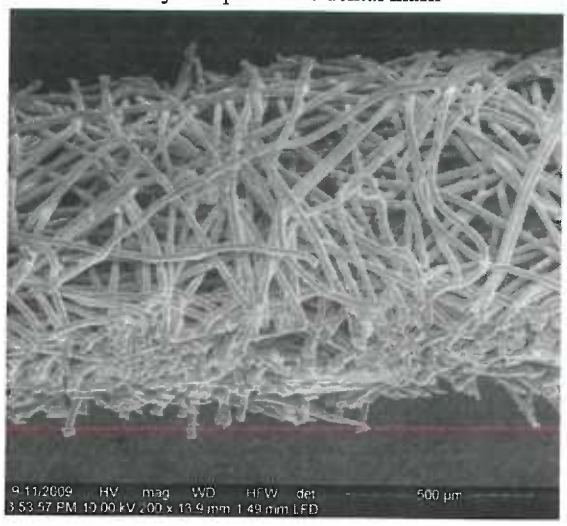

Figure 30. Scanning electron microscopy cross section view of cone dental mask

Discussion:

Mask Comparison

When comparing the procedure mask to the cone mask, results of this study showed that the procedure mask filtered significantly more Transbond particles than the cone mask. The cone mask allowed 1-2.5% of the particles generated to pass, while the procedure mask allowed 0.03-0.06% of the particles generated to pass through to the impactor stages. When compared to the control, the procedure mask reduced the collected dust mass by over 99%, while the cone mask reduced the collected dust mass by 84%. This is far greater than the percentages that have been reported in the literature of 70-80% (Brune and Beltesbredde, 1980b, Harrel and Molinari, 2004). Reasons for the higher percentage may include: a complete seal around the intake port so that no dust may enter the Cascade Impactor without passing through the mask, an overloading of the mask's pores acting to increase filtration ability, types of masks used, or air flow dynamics inherent to the internal air flow within the collection chamber. In a clinical sitting, the particles will likely flow around the mask as well as through the masks due to the inability of most masks to fit accurately (Oberg and Brosseau, 2008).

Of the total particles generated in the controls, at least 4.4% of the particles by mass were aerodynamically respirable. This percentage is less than that found by Collard et al (1991), who reported 14-22% of the dust generated was aerodynamically respirable. This difference may be related to the inaccuracy of the impactor. Using the information from the Microtrac S3500, we can conclude that there was actually a greater number of particles than stated in the aerodynamically respirable range for all samples collected. The difference may also be related to the composites analyzed. Collard et al. (1991) analyzed restorative composites having much greater filler particle size ranges and filler

percentages than those found in the orthodontic adhesive composite analyzed in the present study.

Of the total particles collected in the impactor, at least 19.1% of the particles by mass were aerodynamically respirable when the procedure mask was used, while at least 39.1% of the particles collected were aerodynamically respirable when the cone mask was used. The masks were able to considerably reduce the particles collected, but were less effective in reducing the amount of particles smaller than 2 μm, especially in the case of the cone mask. The ability of the smaller particles to pass through the cone mask represents a significant shortfall of the mask's ability to protect users from the most potentially harmful particle fractions, and in this respect the procedure mask performed better. While these masks do show the ability to limit dust exposure to the respiratory tract, and therefore limit dust ingestion, the N95 mask is the only mask in this experiment which completely blocked all particles from entering the impactor.

In the present study, over 80% of the dust mass generated inside the testing chamber never reached the impactor and remained within the testing chamber. Reasons for this include: 1) uncollected dust was too massive to remain airborne long enough to enter the impactor at the evacuation speeds employed, 2) particles escaped through the ventilation port (present to maintain atmospheric pressure), 3) adhesion to the glove entry ports or the walls of the chamber, and 4) clumping with other particles creating larger and more massive, collective particles. A combination of all of these scenarios is likely.

Estimated Number of Particles:

Even though only a small percentage of the total mass of the generated dust was of very small size, the amount corresponds to an enormous number of particles. In the

control samples, an estimated 6.5×10^9 particles of aerodynamically respirable dust were collected. This data suggests that an estimated average of 6.5×10^9 particles had the potential to penetrate the body's normal defense mechanism and settle in the lungs. However, it should be kept in mind that the average starting sample size had a mass of about 4 g. This is a far greater amount of composite adhesive than an operator would expect to grind from one patient. This amount was used in this study to ensure that enough dust was generated to collect and accurately analyze. However, an estimate of 80 mg may be clinically more relevant. Using the data from this study, one can extrapolate that an exposure in the order of 1.3×10^8 particles is possible, and may represent a potential to cause harm. In addition, the inefficacy of the impactor to accurately separate the particles according to size range reduces the precision produced by the formula to calculate the number of particles in each size range. However, using the information from the Microtrac S3500, we can conclude that there was actually a greater number of particles than stated in the aerodynamically respirable range for all samples collected.

SEM of Masks:

The procedure mask consists of three separate layers, which would contribute to increased efficiency in filtering particles. Although an individual particle could maneuver through the first layer, the second and third layers appear to prevent the majority of the particles from progressing further. In addition, the flatter fibers in the procedure mask would increase the surface area from the direction the particle would be entering. The SEM images show more open spaces on the cone mask when compared to the procedure dental mask. The smaller spaces between the fibers and the layered design

of the procedure mask, as viewed in the SEM, likely explains in part the increased efficiency of the procedure mask to filter the particles.

Accuracy of 8-Stage Impactor

Results of the study showed that the Cascade Impactor does not as accurately separate airborne particles into aerodynamic size classes as claimed by the manufacturer. Analysis of the aluminum oxide particles showed that 2.8% of the total mass collected from the 0.3 μm sample were collected in the expected stage, while 9.5% of the 1 μm particles and 31.58% of the 5 μm particles were collected in the expected stages. Although each sample almost certainly had a distribution of particles slightly larger and smaller than the designated particle size, one would expect better separating accuracy from the impactor. When the aluminum oxide particles were collected with a mask over the intake, mass percentages of the 0.3 μm and 1 μm particles improved to 18.75% and 25.13% in the expected stages, while the 5 μm particle sample showed a result similar to that found without the mask (29.31% in the expected stage).

Furthermore, the Microtrac S3500 showed a significantly different result from the impactor in terms of particle sizes when comparing the same sample. When evaluating the composite particles collected without a mask over the intake, only stages 1, 3 and 6 were statistically equivalent. Although the SEM showed a difference in particles between the different stages, the impactor was unable to accurately segregate particles according to stage as claimed by the manufacturer. The SEM measurements correlate much closer to the results from the Microtrac S3500.

For the Cascade Impactor to function properly, particles must enter each stage without being attached to other particles. Aerosolizing charged particles likely leads to

agglomeration of the particles before entering the impactor or while progressing through the stages of the impactor. If particles are clumped together, the particles would impact on an earlier stage than would happen if each particle were dissociated and acting independent from other particles. In addition, with so many particles entering the impactor, unavoidably particles will collide, which also may prevent the particles from impacting on the correct stage plate. This would explain the improvement in accuracy of the aluminum oxide particles with the mask over the intake. The mask would limit the number and reduce the flow of particles (especially the larger particles) entering the impactor and thereby allow more free movement of particles as they flowed through the stages of the impactor. Other contributing factors may include manufacturing variability and susceptibility to wear-induced changes in the stage cut points (Stein and Olson, 1997, Marple et al., 1998).

Biological Significance:

To date, no reported cases of pulmonary damage due to dental composites have been found in the orthodontic literature despite the exposure potential this study has demonstrated. Several factors beyond the scope of this study may be related to this phenomenon, foremost being the aerodynamically respirable dust distribution in a clinical setting. This study was conducted in a closed environment in order to maximize dust collection, whereas in a clinical setting, the dust would be free to distribute into a much larger volume of air. This fact may greatly limit exposure and allow the aerodynamically respirable particles to settle out onto clinic surfaces, later to be removed during house cleaning procedures or by the facility's air ventilation system. The use of high volume evacuation also would decrease the amount of particles if used in a clinical environment.

Conversely, these same systems may also be acting to maintain aerodynamically respirable dust in the air, allowing for secondary contamination of others within the clinic not directly involved with the debonding procedures.

Another limitation of the study design is the role of chairside vacuum systems on the dust that is generated. As Brune and Beltesbredde (1980b) and Collard et al (1991) point out, typical chairside vacuum systems operate at only 16% of the evacuation efficiency that they consider adequate. Further studies should focus on the effects of air evacuation systems on the quality and quantity of dust that escapes retrieval. Another concern is the patient's exposure to aerodynamically respirable dust. Being an acute, relatively low dose exposure it may be unlikely the individual patient is at any health risk. Another factor may be humidity in the pulmonary system (or humidity in the environment) preventing particles from staying airborne. Further, the patient's acute exposure may actually reduce the total aerodynamically respirable dust load released into the environment, and limit the chronic exposure to the operator.

From a mechanical standpoint, this study used a Cascade Impactor to collect and fraction dust particles into stages that theoretically correspond to pulmonary penetration depths. In order for this machine to function properly a constant vacuum must be maintained, a situation that does not resemble the human respiratory system functions. Aerodynamically respirable dust particles that are inhaled may also be exhaled. Without human studies, the true level of retention of aerodynamically respirable dust cannot be determined. However, animal studies suggest that some level of retention is likely (Gross et al., 1970). This leads us to ponder one additional limitation of this study, i.e. the human body's capacity for removal of this aerodynamically respirable dust. Is typical exposure to aerodynamically respirable dust through orthodontic procedures simply

insufficient to overwhelm the body's ability to remove these particles, irrespective of the fact that it contains quartz, a known cancer causing agent? As efficiency improves the clinician's ability to treat patients, some practices are able to see 100 or more patients per day. Does this mean it is only a matter of time before reports of respiratory ailments due to aerodynamically respirable dust exposure will begin to surface? Either way, the potential for a human health risk is clear and further research is required

Conclusions

Results of the study showed that the Cascade Impactor does not accurately separate airborne particles into aerodynamic size classes, as claimed by the manufacturer. Based on a comparison with a laser-based particle size analyzer and scanning electron microscopy, it is likely that the Cascade Impactor underestimates the amount of respirable particles. In consideration of this limitation, the following conclusions are made:

1. Use of a procedure dental mask reduced the amount of dust mass that would normally be inhaled by 99%. Use of a cone dental mask reduced the amount of dust mass by 84%. Use of an industrial particulate respirator, the N95 mask, reduced the amount of dust mass by 100%.
2. Of the dust particles collected when using the procedure dental mask, at least 19.1% by mass was considered to be aerodynamically respirable, based on the

impactor results, while at least 39.1% by mass was considered to be aerodynamically respirable when using the cone dental mask.

3. The average aerodynamically respirable dust collected from the procedure dental mask samples was estimated to contain at least 6.95×10^7 particles, according to the results from the impactor, while the average aerodynamically respirable dust from the cone dental mask samples was estimated to contain at least 4.43×10^8 particles.
4. This study illustrates a potential exposure to aerodynamically respirable dust that contains quartz from the grinding of quartz containing composite adhesives used in orthodontics. The procedure dental mask performed better than the cone dental mask at filtering these particles. However, only the N95 mask blocked all particles from entering the impactor.

Recommendations

Until further research shows the exposure amount of particles that will cause pathology, the following recommendations are made:

1. Due to the potential exposure to aerodynamically respirable dust, the N95 mask is suggested to completely filter the particles.
2. The increased cost and decreased comfort of the N95 masks make the routine use of N95 masks impractical. Therefore, a mask with a filtering ability at least as good as the procedure mask is recommended for debonding appointments, along with high volume evacuation to minimize the entry of potential respirable dust.

Future Studies

In consideration of the limitations of this study, the following is suggested in considering future studies:

1. Evaluating the fit of masks to evaluate how many particles can potentially enter the pulmonary system around the mask.
2. Animal studies to determine the extent to which the pulmonary system eliminates these particles.
3. Studies to determine the efficiency of dental evacuation systems to determine the quality and quantity of dust that escapes retrieval. Use high volume evacuation inside the testing apparatus during the grinding process to see if any particles make it to the impactor stages.

ACKNOWLEDGEMENTS

Thank you to my thesis mentor, Dr. Jack Ferracane, for guiding and advising me throughout the project.

Thank you to Dr. Matt Almeida for developing the protocol, collecting data and taking photos used in this project.

Thank you to my thesis committee members, Dr. David Covell and Dr. Larry Doyle, for suggestions and reviewing drafts.

Thank you to Dr. Xiaoming Xu and Dr. Yuwei Fan for performing the laser particle analysis.

Thank you to Dr. John Mitchell and Dr. Katie Clark for assistance in operating the scanning electron microscope.

Thank you to my wife, Angela, and my children, Kyra and Ian, for their support.

Appendix A:

Ambient (non-viable) 8-stage Cascade Impactor:

The Ambient Eight-Stage Cascade Impactor (Fig. 31) used in this experiment is a high sample-rate, multiple orifice and multiple stage inertial impactor. A Cascade Impactor is a multi-stage device used to separate airborne particles into aerodynamic size classes. The Impactor is fabricated from an aluminum alloy. It is designed to aerodynamically separate ambient particulate into multi fractions in the range of 10 μm AED (Aerodynamic Equivalent Diameter) to filtration collection of sub-micron particles down to less than 0.43 μm.

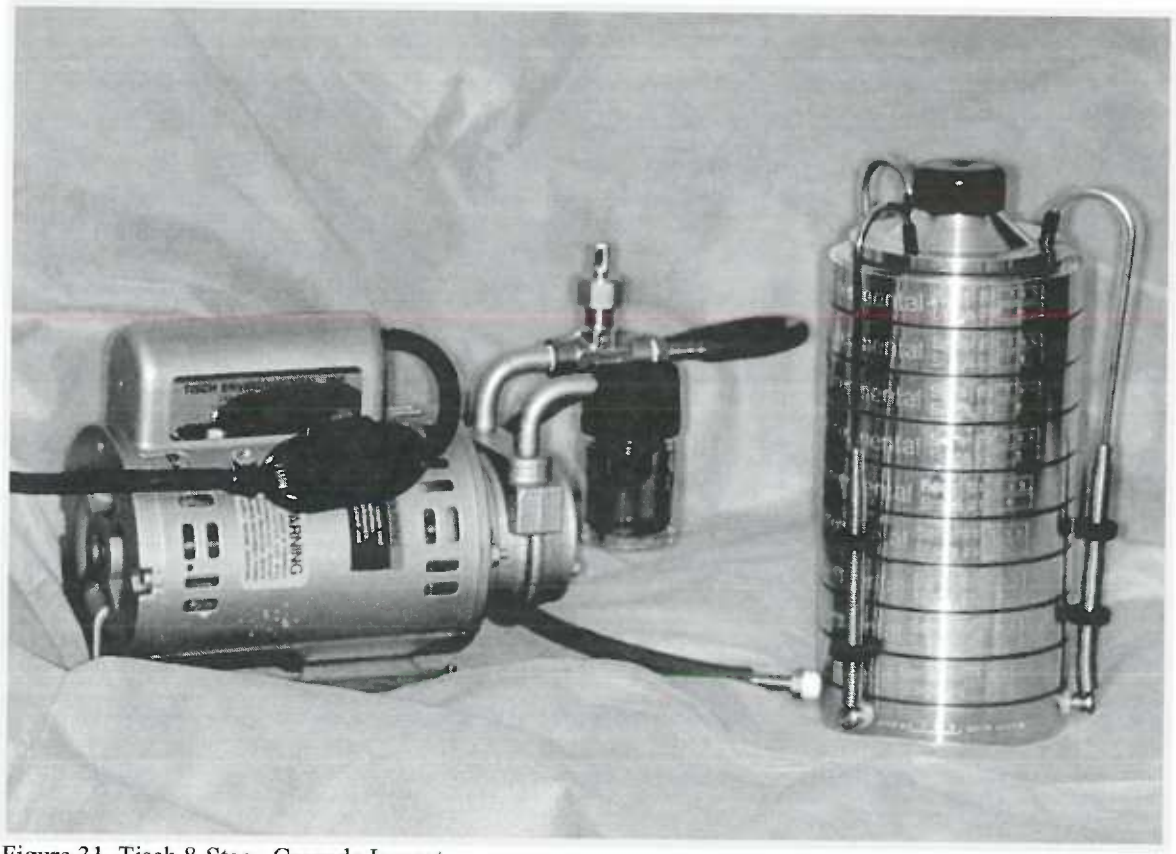

Figure 31. Tisch 8-Stage Cascade Impactor

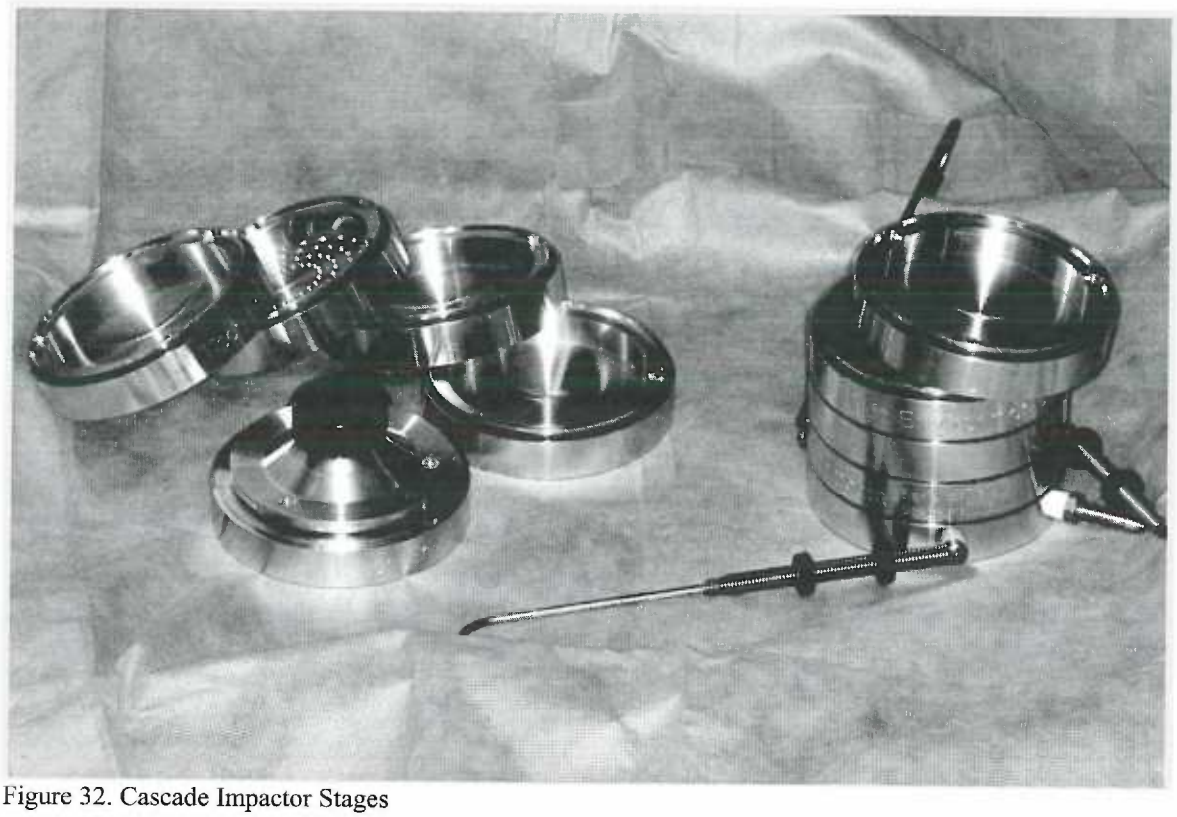

Figure 32. Cascade Impactor Stages

Within the Impactor, the particulate entrained in the aerosol is sampled through a series of stacked stages which contain multiple orifices with sequentially smaller diameters (Fig. 32). Ambient air enters the circular inlet cone and cascades through the succeeding orifice stages with successively higher orifice velocities from Stage #0 to Stage #7. Successively smaller aerodynamic sized particles are impacted by inertia onto a collection medium. The sub-micrometer particles (<1.0 μm) passing through Stage #7, are collected by filtration on a glass micro-fiber or cellulose filter media. The sampled air is drawn through the Cascade Impactor using a calibrated vacuum pump designed to maintain a constant sample rate. The design sample flow rate of the Eight Stage Ambient Cascade Impactor is ALPM (actual liters/minute) or 1 cubic foot/minute. A sample flow rate of 28.3± 1.5 ALPM during a sample event ensures the aerodynamic separation of particles maintain the theoretical calibration curves.

This model 20-800 series of Cascade Impactors is designed for applications in ambient air where non-viable (non-biological) aerosol is to be collected and measured for its concentration by aerodynamic particle size. The concentration of particulate is calculated by pre and post weighing of the 81 mm sample substrates located below each Orifice Stage. As particles pass through each successively smaller diameter orifice stage the sample is accelerated. As the aerosol exits each orifice it will curve around the impaction sample substrate. Particles that have an aerodynamic diameter and inertia that cannot stay in the sample air stream (because they are too large) break free from the flow and collect by impaction onto the sample substrate. By subsequently making the orifice diameter smaller on each Stage of the Cascade Impactor, the particles are progressively increased in velocity and the sequential aerodynamic separation of smaller and smaller particles can be determined over a fairly large range.

Dr. K. R. May, Ph.D, introduced the first commercial Cascade Impactor in 1945 in the United Kingdom and published its design and function in the Journal of Scientific Instruments (May, 1945). The design uses a single orifice jet impacting onto a glass microscope slide and four successive Stages with decreasing orifice diameters. The "May Impactor" remains a valuable laboratory tool even today with well-characterized and precise particle separation efficiency. Its only limitation is the sample flow rate is low and the glass slides require grease-coatings to collect the sample for analysis.

The Ambient Eight-Stage Cascade Impactor concept was designed and published by Dr. Aerial Andersen in Provo, Utah in 1958 (Andersen, 1958). In an attempt to improve collection efficiency Dr. Andersen developed the multiple stage, multiple-orifice Cascade Impactor. The unique design of multiple orifice jets in one stage allowed for higher sampler flow rates and a larger sample substrate to collect greater mass

concentration for weighing accuracy and later chemical speciation analysis. The design has been utilized by many researchers in the environmental, industrial hygiene and pharmaceutical industries for thirty years and has been extensively tested and verified for characterization. Several commercial copies of the original design are being fabricated today.

Appendix B:

Log Probability Graphs

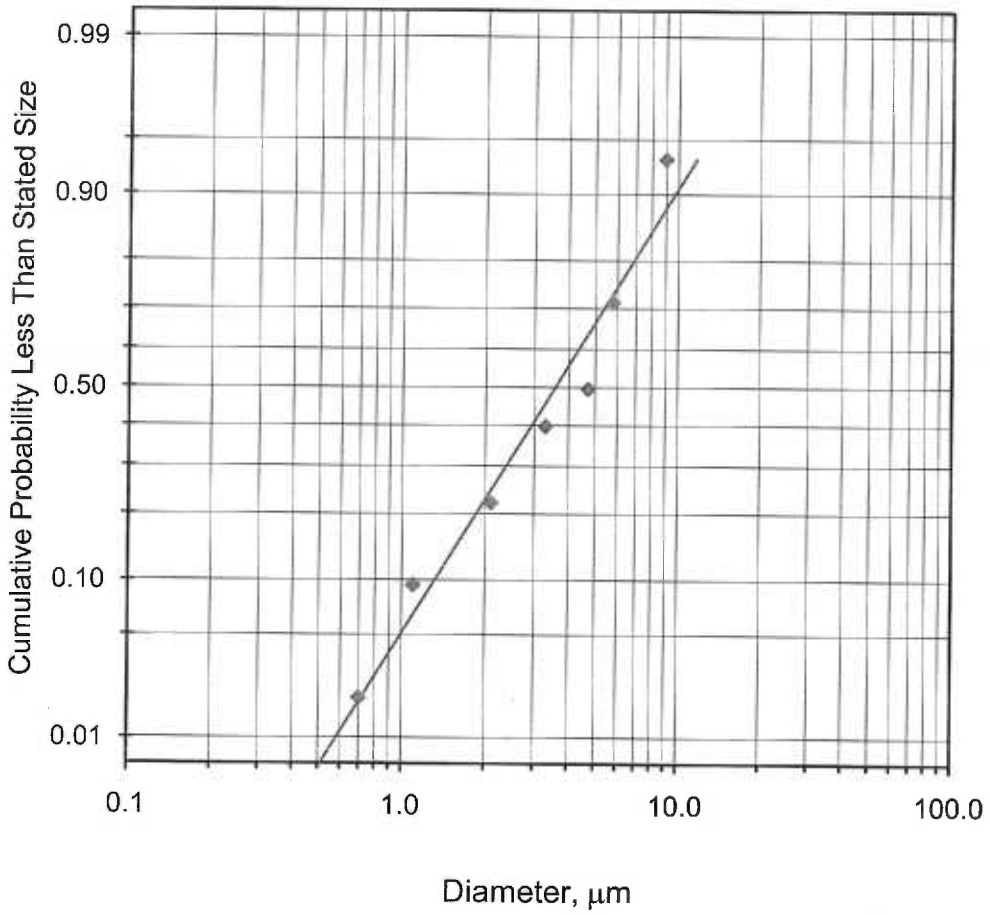

Figure 1. Log Probability graph: Cone Dental Mask Trial #1 with cumulative probability less than stated size plotted against diameter in microns; MMAD = 4.39 μm, Geometric Std. Dev = 2.4, Concentration = .01 mg/m³

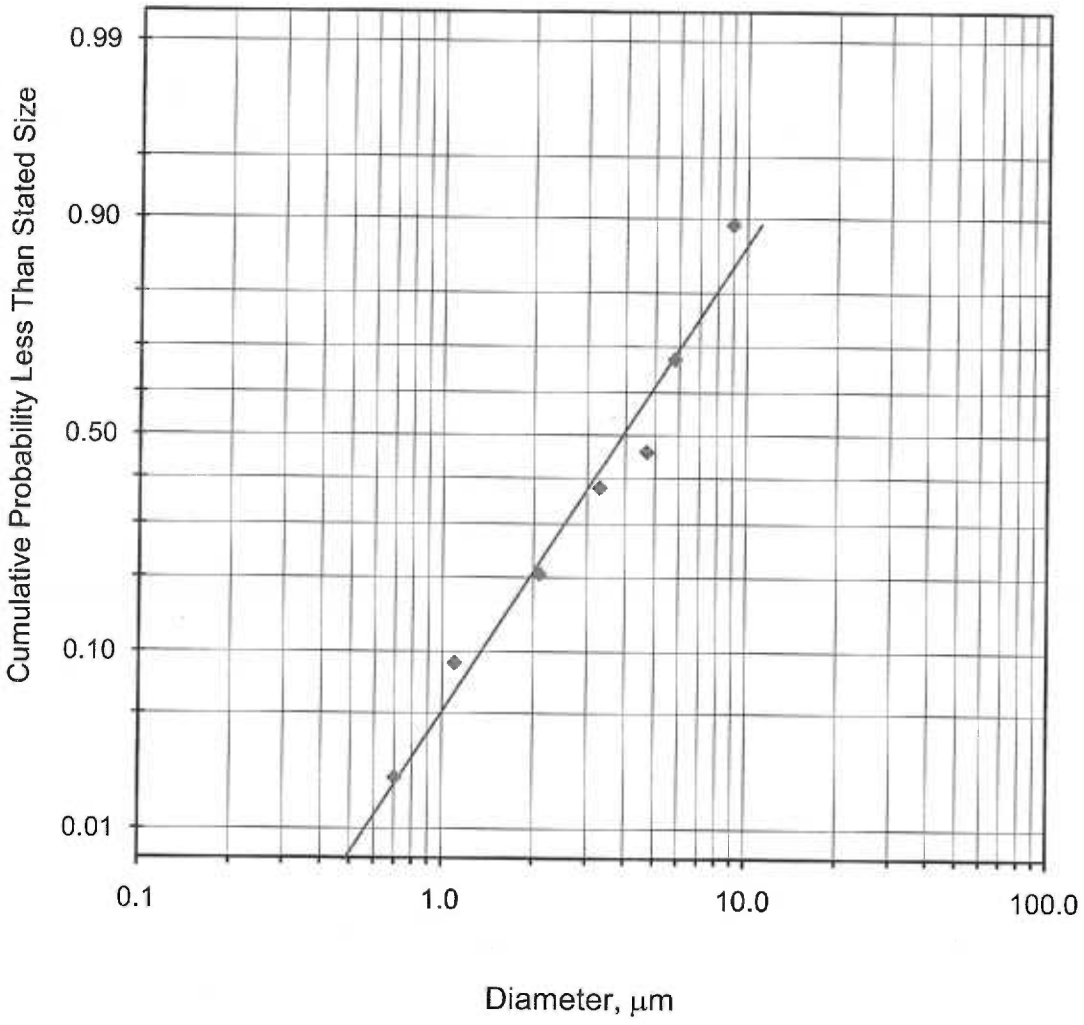

Figure 2. Log Probability graph: Cone Dental Mask Trial #2 with cumulative probability less than stated size plotted against diameter in microns; MMAD = 3.93 μm, Geometric Std. Dev = 2.31, Concentration = .02 mg/m³

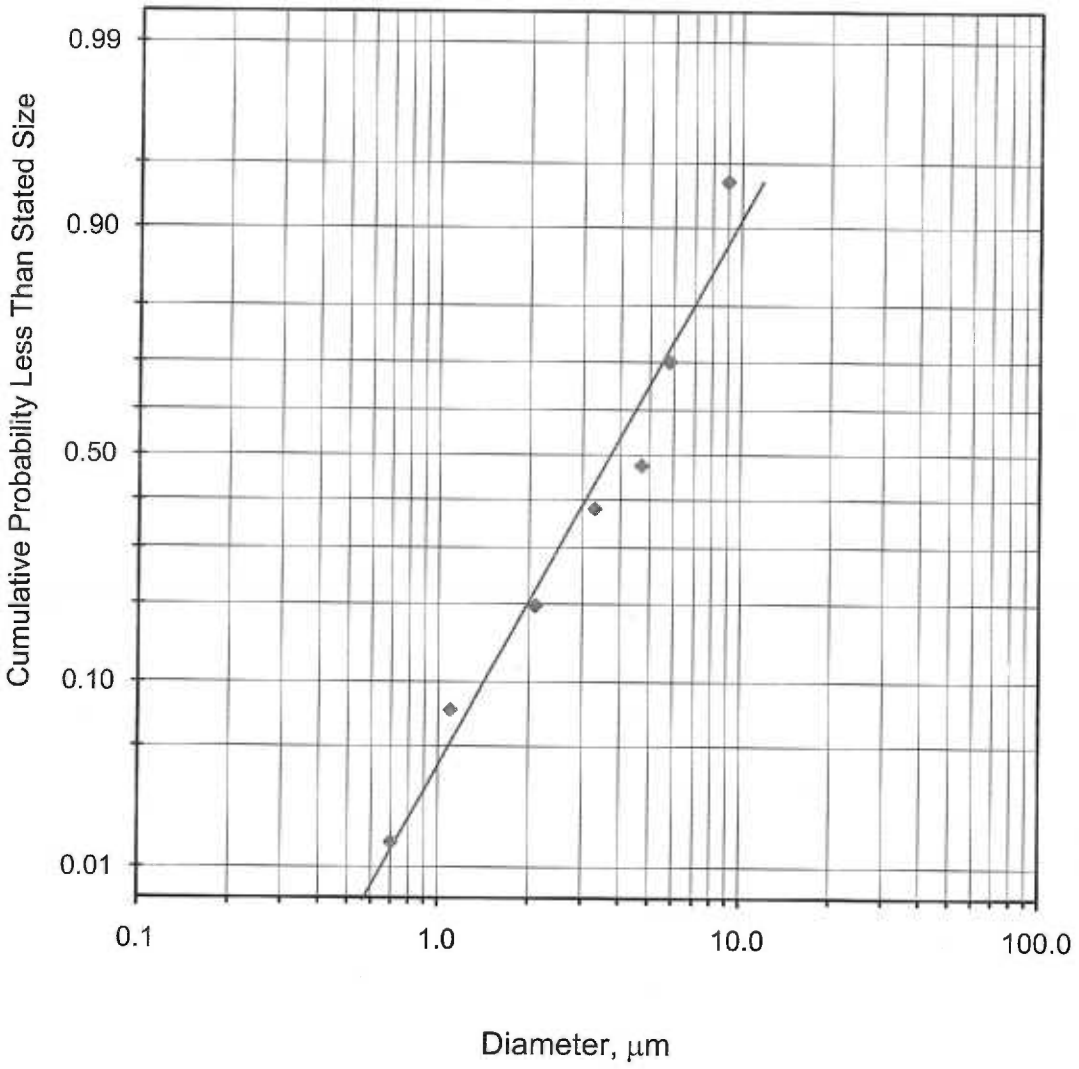

Figure 3. Log Probability graph: Cone Dental Mask Trial #3 with cumulative probability less than stated size plotted against diameter in microns; MMAD = 3.71 μm, Geometric Std. Dev = 2.11, Concentration = .03 mg/m³

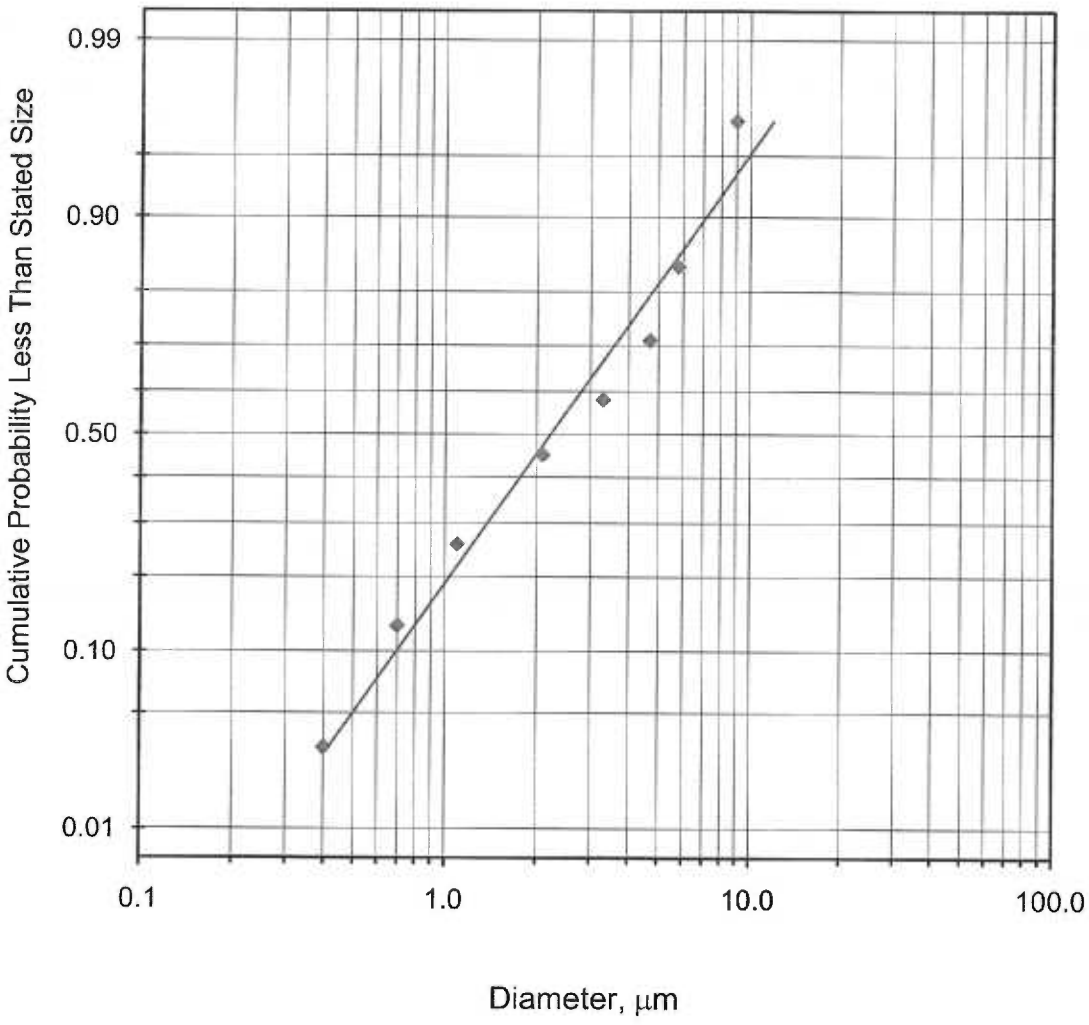

Figure 4. Log Probability graph: Procedure Dental Mask Trial #1 with cumulative probability less than stated size plotted against diameter in microns; MMAD = 2.23 μm, Geometric Std. Dev = 2.48, Concentration = .00091mg/m³

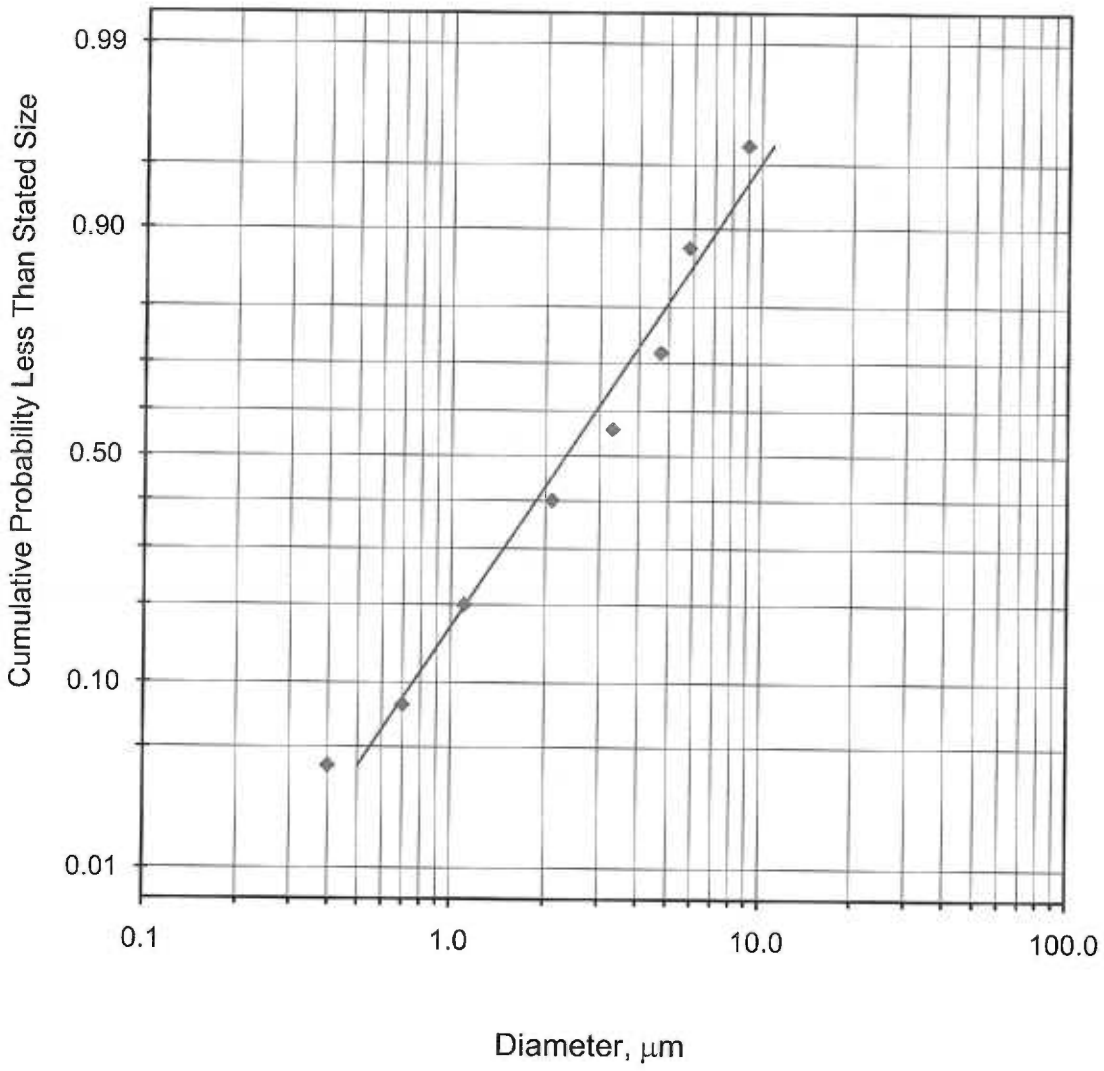

Figure 5. Log Probability graph: Procedure Dental Mask Trial #2 with cumulative probability less than stated size plotted against diameter in microns; MMAD = 2.33 μm, Geometric Std. Dev = 2.41, Concentration = .00074mg/m³

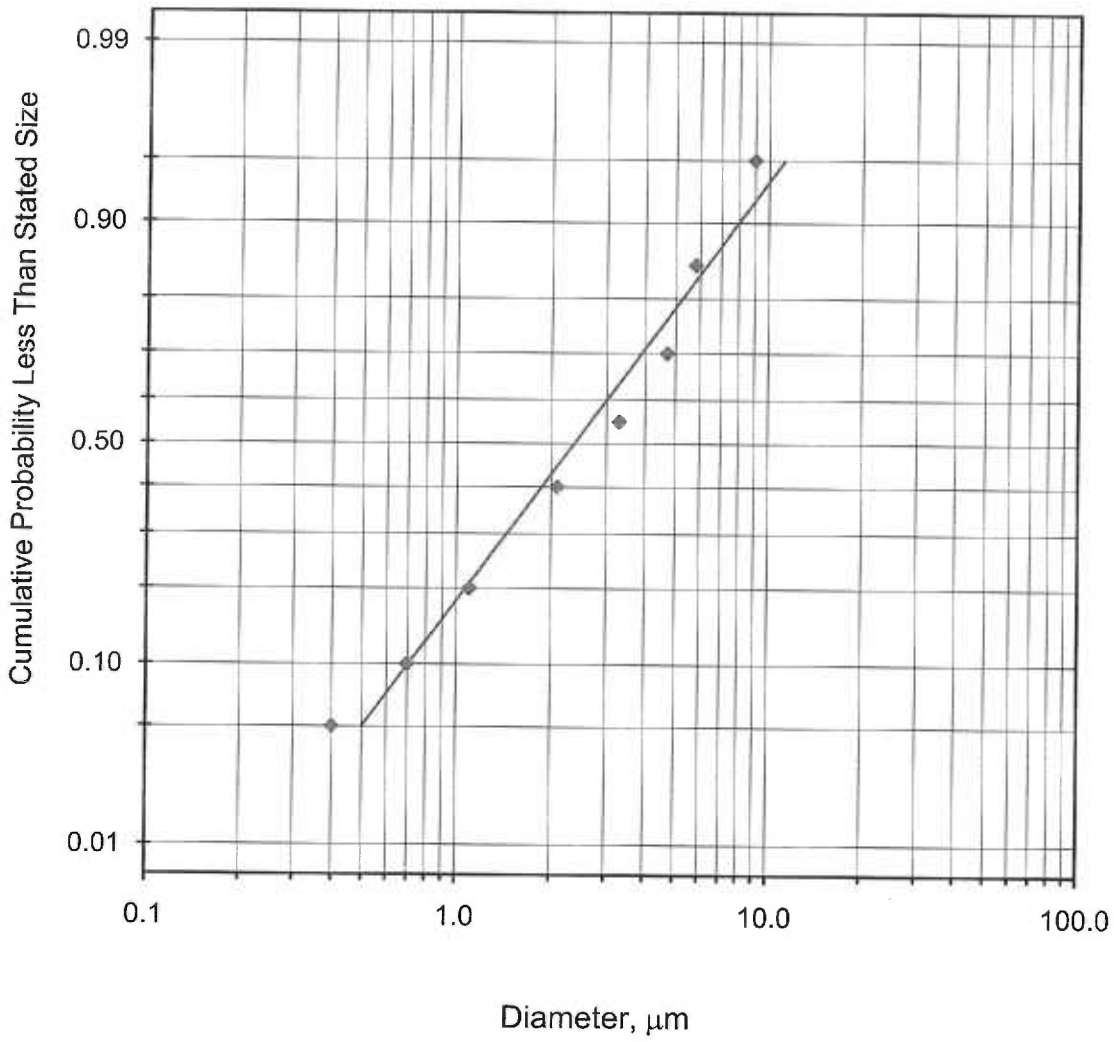

Figure 6. Log Probability graph: Procedure Dental Mask Trial #3 with cumulative probability less than stated size plotted against diameter in microns; MMAD = 2.37 μm, Geometric Std. Dev = 2.57, Concentration = .00059 mg/m³

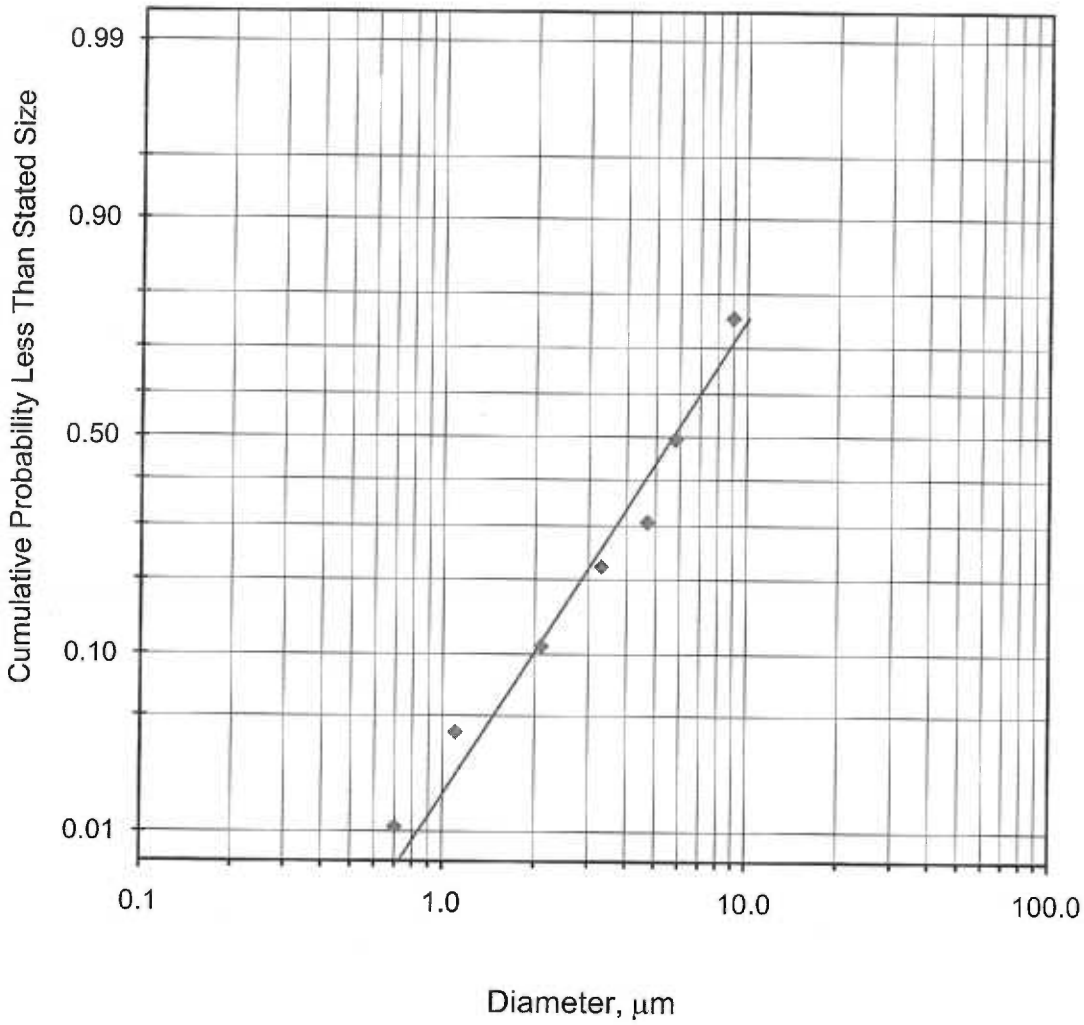

Figure 7. Log Probability graph: Control Trial #1with cumulative probability less than stated size plotted against diameter in microns; MMAD = 5.69 μm, Geometric Std. Dev = 2.28, Concentration = .09 mg/m³

Appendix C:

Comparative Statistic Charts

Table I. ANOVA: Single Factor Comparing Total Mass collected with Procedure mask and Cone mask to Control

SUMMARY

Groups	*Count*	*Sum*	*Average*	*Variance*
Column 1	3	0.1998	0.0666	0.00023877
Column 2	3	0.0049	0.001633	3.03333E-07
Column 3	3	0.608	0.202667	0.000817203

ANOVA

Source of Variation	*SS*	*df*	*MS*	*F*	*P-value*	*F crit*
Between Groups	0.063149	2	0.031575	89.67708271	3.39193E-05	5.143253
Within Groups	0.002113	6	0.000352			
Total	0.065262	8				

Table II. ANOVA: Single Factor Comparing Mass Colleced in Impactor as a Percentage of Total Mass Ground with Procedure Mask (column 1) and Cone Mask (column 2) and No Mask (column 3)

SUMMARY

Groups	*Count*	*Sum*	*Average*	*Variance*
Column 1	3	0.0013	0.000433	2.33E-08
Column 2	3	0.0501	0.0167	1.75E-05
Column 3	3	0.4011	0.1337	0.001312

ANOVA

Source of Variation	*SS*	*df*	*MS*	*F*	*P-value*	*F crit*
Between Groups	0.031713609	2	0.015857	35.77844	0.000463	5.143253
Within Groups	0.002659167	6	0.000443			
Total	0.034372776	8				

Table III. ANOVA Two-Factor With Replication: Mask Type vs. Stage #(Mass Percent)

Two Way Analysis of Variance Sunday, September 27, 2009, 12:00:55 PM

Balanced Design

Dependent Variable: Col 3

Normality Test: Passed (P = 0.066)

Equal Variance Test: Passed (P = 0.848)

Source of Variation	**DF**	**SS**	**MS**	**F**	**P**
Col 1	1	0.00000000120	0.00000000120	0.00000186	0.999
Col 2	7	0.266	0.0380	58.815	<0.001
Col 1 x Col 2	7	0.0928	0.0133	20.521	<0.001
Residual	32	0.0207	0.000646		
		Total 47	0.379 0.00807		

Table IV. ANOVA Two-Factor With Replication: Mask Type vs. Stage #(Mass)

SUMMARY	1	2	3	4	5	6	7	8	Total
mask 1									
Count	3	3	3	3	3	3	3	3	24
Sum	0.0537	0.0472	0.0208	0.0387	0.0247	0.0121	0.0024	0.0002	0.1998
Average	0.0179	0.015733	0.006933	0.0129	0.008233	0.004033	0.0008	6.67E-05	0.008325
Variance	0.00000199	7.09E-06	3.86E-06	1.9E-05	1.01E-05	2.97E-06	1.2E-07	1.33E-08	4.47E-05
mask 2									
Count	3	3	3	3	3	3	3	3	24
Sum	0.0005	0.0008	0.0008	0.0008	0.0012	0.0006	0.0002	0	0.0049
Average	0.00016667	0.000267	0.000267	0.00027	0.0004	0.0002	6.67E-05	0	0.000204
Variance	1.3333E-08	3.33E-09	3.33E-09	3.3E-09	1E-08	1E-08	1.33E-08	0	1.95E-08
Total									
Count	6	6	6	6	6	6	6	6	
Sum	0.0542	0.048	0.0216	0.0395	0.0259	0.0127	0.0026	0.0002	
Average	0.00903333	0.008	0.0036	0.00658	0.004317	0.002117	0.000433	3.33E-05	
Variance	9.5143E-05	7.46E-05	1.49E-05	5.5E-05	2.24E-05	5.6E-06	2.15E-07	6.67E-09	

Anova: Two-Factor With Replication Mask Type vs. Stage #

Source of Variation	*SS*	*df*	*MS*	*F*	*P-value*	*F crit*

Sample	0.00079138	1	0.000791	281.107	2.09E-17	4.149097
Columns	0.00047826	7	6.83E-05	24.2694	4.23E-11	2.312741
Interaction	0.00046012	7	6.57E-05	23.3488	7E-11	2.312741
Within	9.0087E-05	32	2.82E-06			
Total	0.00181985	47				

Table V. ANOVA Two-Factor With Replication: Mask type(procedure, cone, and no mask) vs. Stage # when comparing the estimated number of particles collected

SUMMARY	1	2	3	4	5	6	7	8	Total
mask 1									
Count	3	3	3	3	3	3	3	3	24
Sum	231000	413000	4E+06	8E+06	28080000	8E+07	9E+07	0	2.09E+08
Average	77000	137667	1E+06	3E+06	9360000	2.7E+07	3E+07	0	8713250
Variance	1.5E+08	9E+08	7E+10	3E+11	5.48E+12	7.8E+13	7E+14	0	2.06E+14
mask 2									
Count	3	3	3	3	3	3	3	3	24
Sum	4880000	1.1E+07	4E+07	2E+08	2.78E+08	5.2E+08	3E+08	4.5E+07	1.35E+09
Average	1626667	3750000	1E+07	6E+07	92800000	1.7E+08	9E+07	1.5E+07	56063750
Variance	3.3E+11	1.4E+12	5E+13	4E+14	9.26E+14	1.4E+15	1E+15	1.7E+14	3.71E+15
Total									
Count	6	6	6	6	6	6	6	6	
Sum	5111000	1.2E+07	5E+07	2E+08	3.06E+08	6E+08	4E+08	4.5E+07	
Average	851833	1943833	8E+06	3E+07	51080000	1E+08	6E+07	7433333	
Variance	8.5E+11	4.5E+12	7E+13	1E+15	2.46E+15	7.1E+15	2E+15	1.3E+14	

ANOVA

Source of Variation	*SS*	*df*	*MS*	*F*	*P-value*	*F crit*
Sample	2.7E+16	1	3E+16	84.331	1.75E-10	4.1491
Columns	5.3E+16	7	8E+15	23.812	5.42E-11	2.31274
Interaction	2.7E+16	7	4E+15	11.982	2.15E-07	2.31274
Within	1E+16	32	3E+14			
Total	1.2E+17	47				

Appendix D:

Additional Figures

Figure 1: Estimated Number of Particles / Stage: Procedure Mask vs. Cone Mask

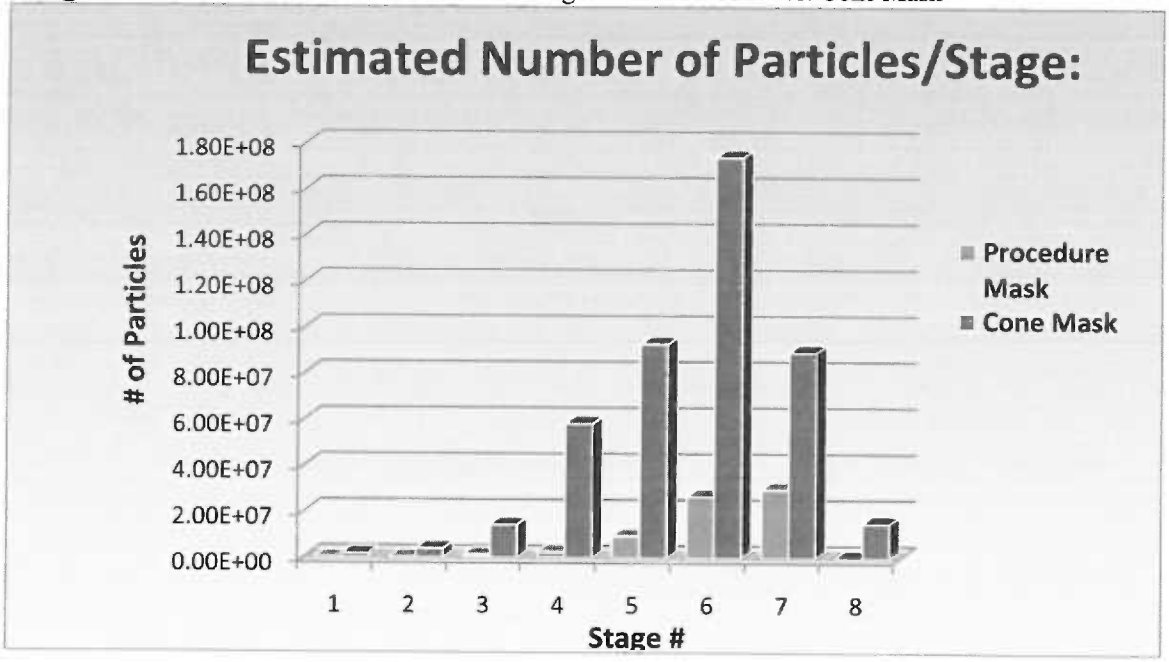

Figure 2: Log Probability Graph: Sample #1 A

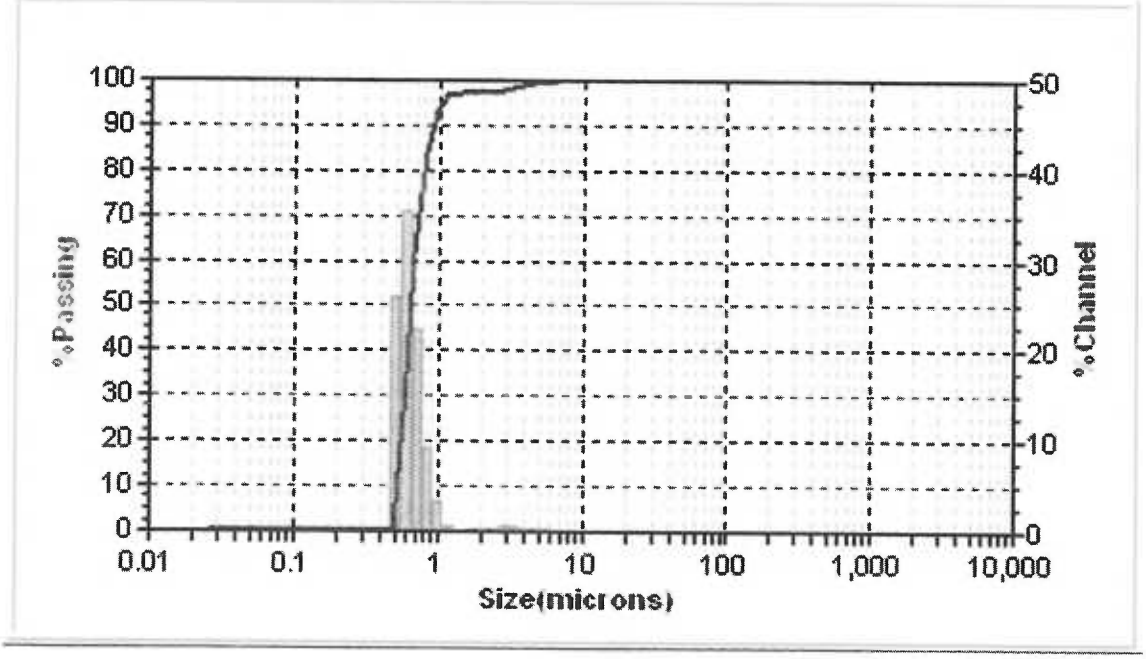

Figure 3: Log Probability Graph: Sample #1 B

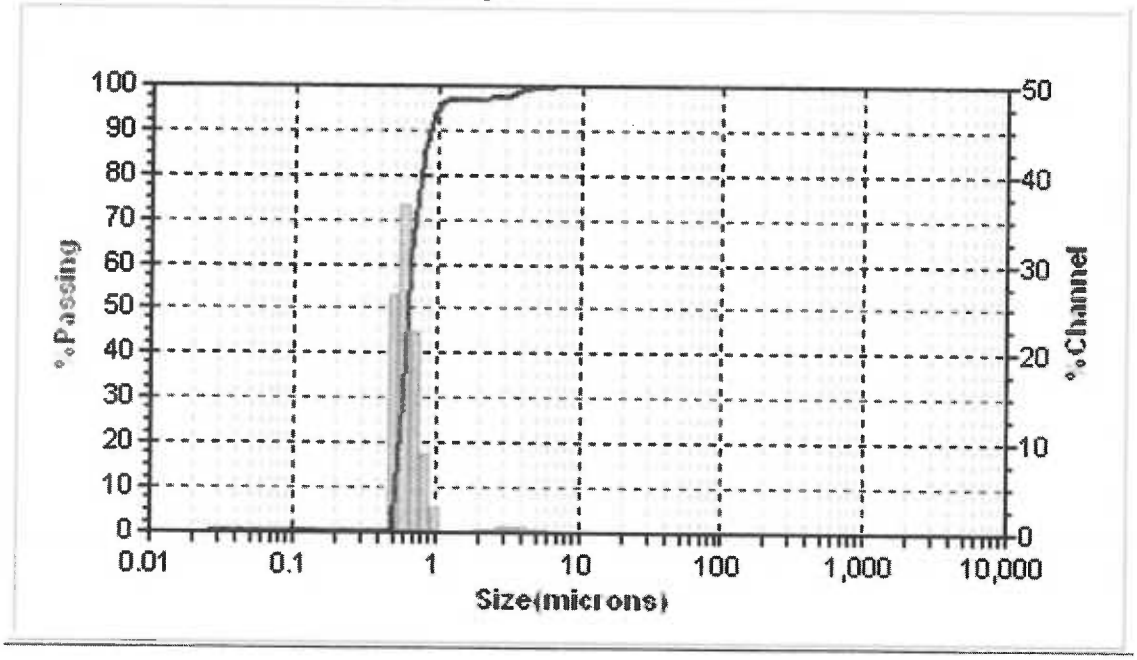

Figure 4: Log Probability Graph: Sample #2 A

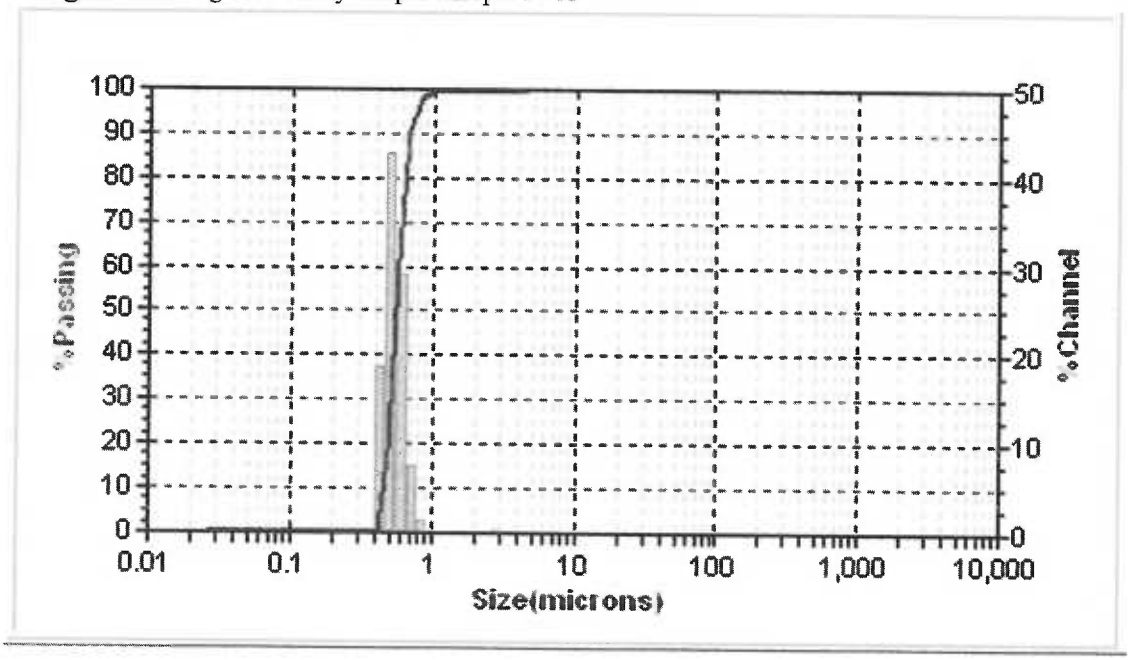

Figure 5: Log Probability Graph: Sample #2 B

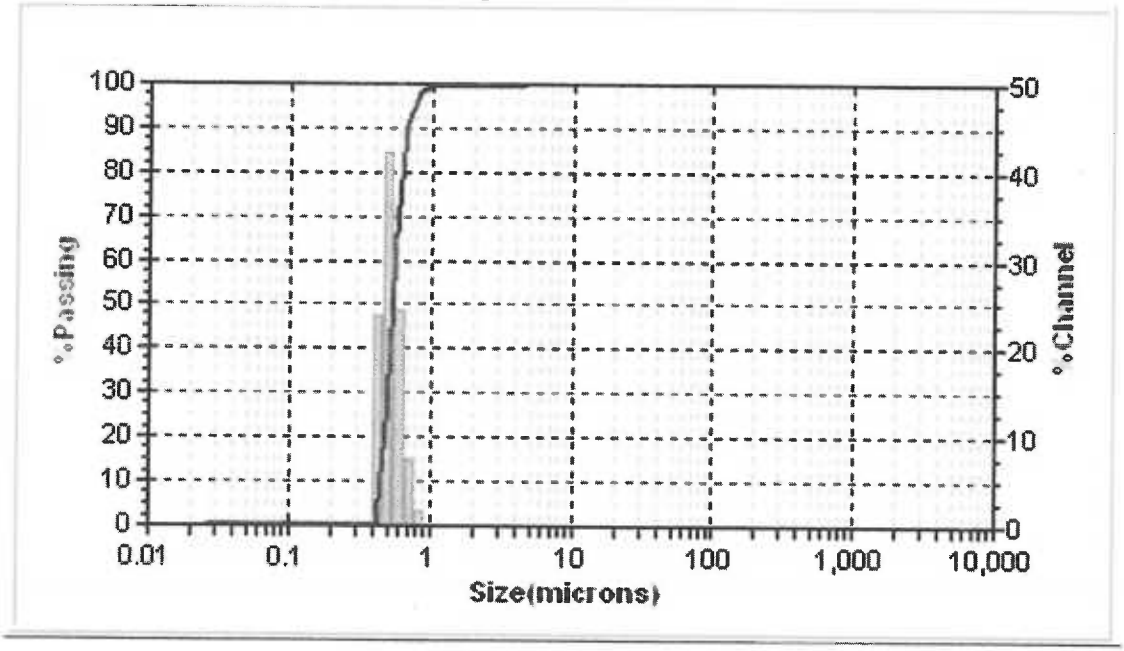

Figure 6: Log Probability Graph: Sample #3 A

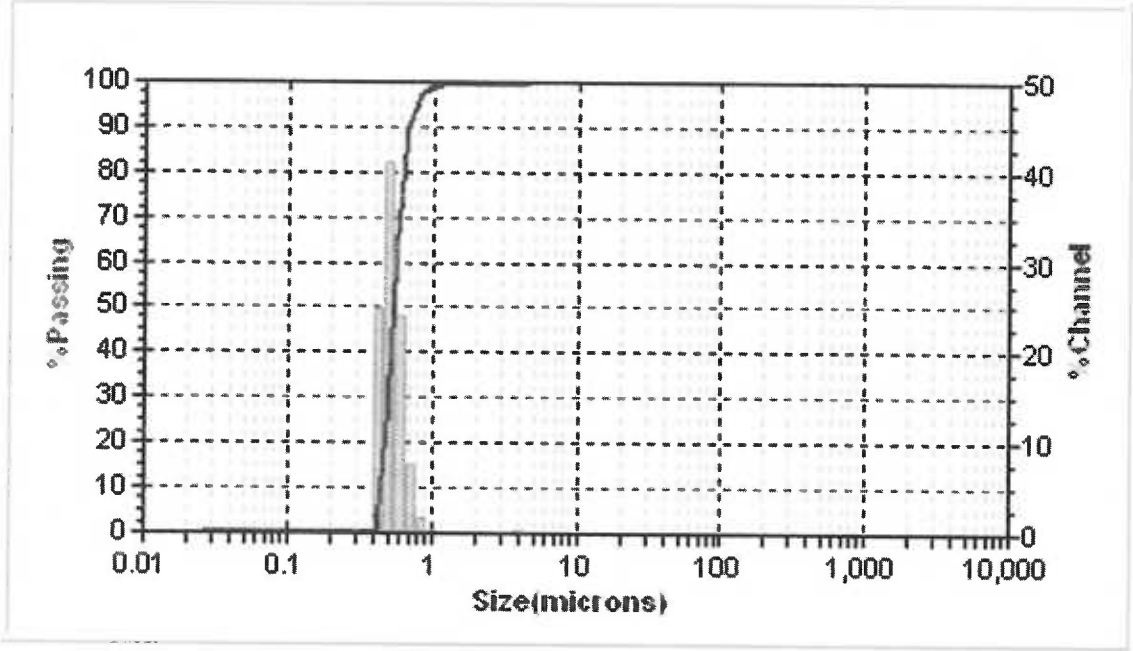

Figure 7: Log Probability Graph: Sample #3 B

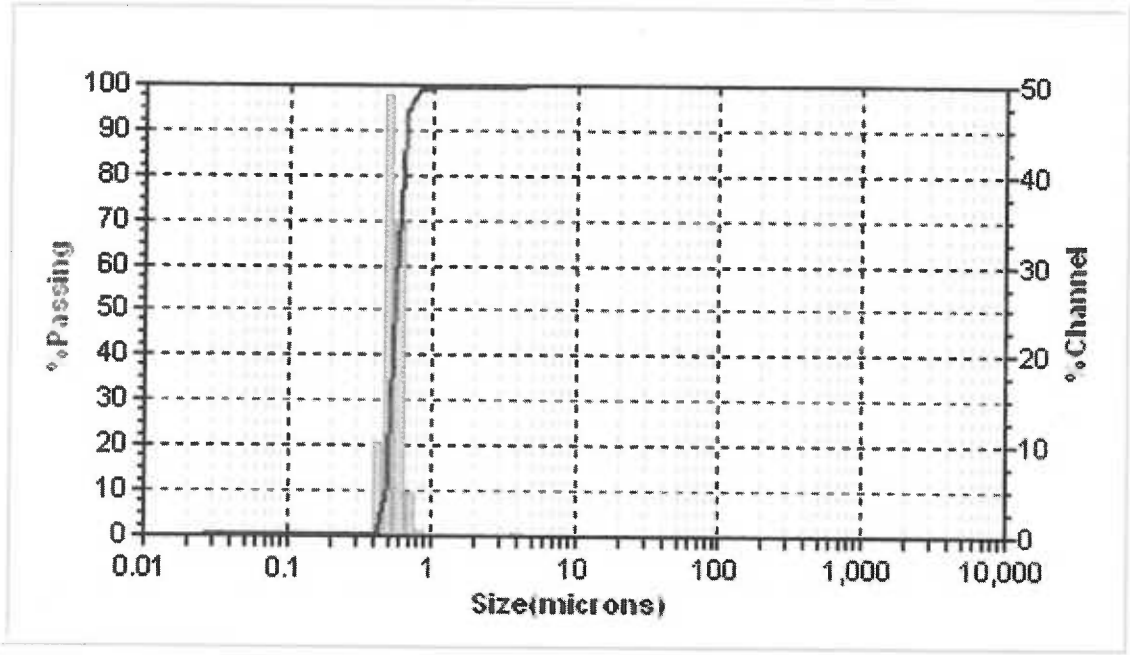

Figure 8: Log Probability Graph: Sample #4 A

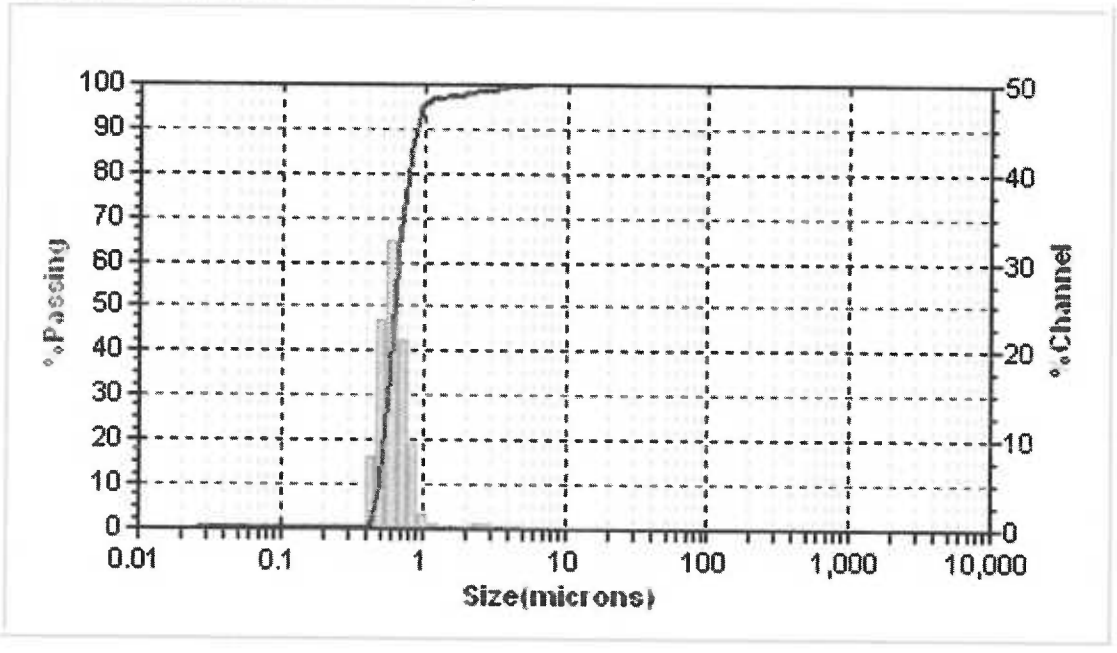

Figure 9: Log Probability Graph: Sample #4 B

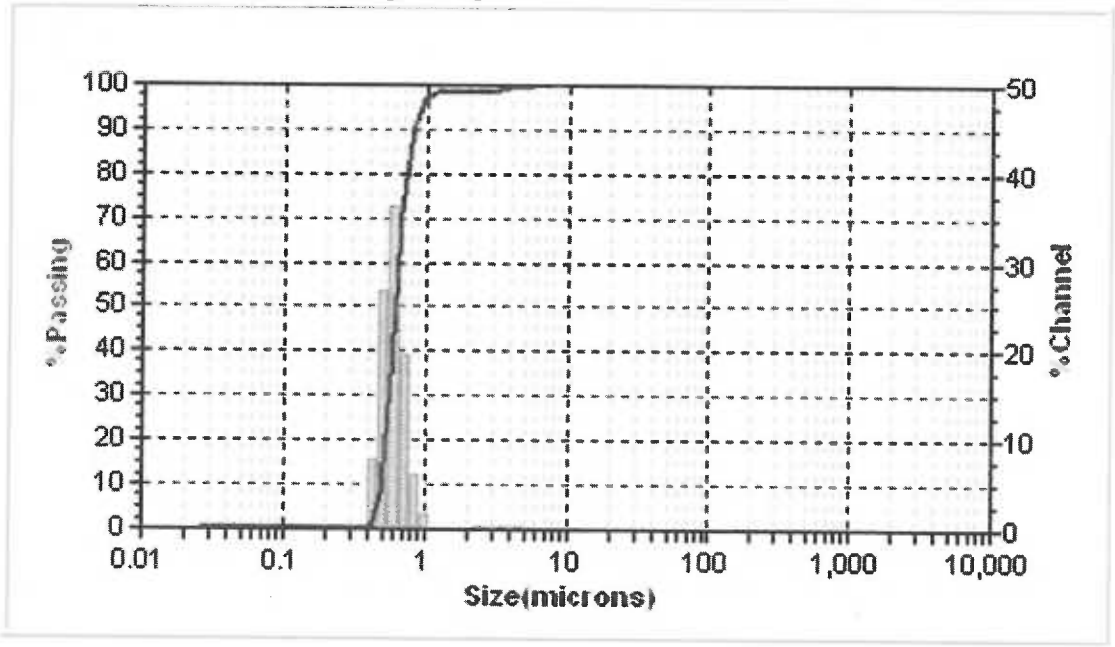

References:

1. Almeida M, Ferracane J, Covell D, Dyer S. Analysis of Aerodynamically Respirable Dust Generated from Air Rotary Abrasion of Quartz Containing Orthodontic and Dental Composites. OHSU Orthodontics Thesis, 2006
2. Andersen A. New sampler for the collection, sizing, and enumeration of viable airborne particles. *J Bacteriol.* 1958;76:471-84.
3. Bello D, Virjo MA, Kalil AJ, Woskie SR. Quantification of respirable, thoracic, and inhalable quartz exposures by FT-IR in personal impactor samples from construction sites. *Appl Occup Environ Hyg.* 2002;17:580-90.
4. Brune D, Beltesbredde H. Dust in dental laboratories. Part I. Types and levels in specific operations. *J Prosthet Dent* 1980a;43:687-692.
5. Brune D, Beltesbredde H. Dust in dental laboratories. Part III: Efficiency of ventilation systems and face masks. *J Prosthet Dent.* 1980b;44:211-5.
6. Chasteen, JE. Four-Handed Dentistry in Clinical Practice, St. Louis, C.V. Mosby Co., 1978.
7. Collard SM, McDaniel RK, Johnston DA. Particle size and composition of composite dusts. *Am J Dent* 1989;2:247-253.
8. Collard SM, Vogel JJ, Ladd GD. Respirability, microstructure and filler content of composite dusts. *Am J Dent* 1991;4: 143-51.
9. Davis LK, Wegman DH, Monson RR, Froines J. Mortality experience of Vermont granite workers. *Am J of Ind Med* 1983;4:702-723.
10. Dufresne A, Lesage J, Perrault G. Evaluation of occupational exposure to mixed dusts and polycyclic aromatic hydrocarbons in silicon carbide plants. Am Ind Hyg Assoc J. 1987;48:160-6.

11. Funahashi A, Schleuter DP, Pintar K, Siegesmund KA. Value of in situ elemental microanalysis in the histologic diagnosis of silicosis. *Chest.* 1984 Apr;85(4):506-9

12. Giodano R. Fiber reinforced composite resin systems. *Gen Dent.* 2000;48:244-9.

13. Greco PM, Lai CH. A new method of assessing aerosolized bacteria generated during orthodontic debonding procedures. *Am J Orthod Dentofacial Orthop.* 2008 Apr; 133:579-87.

14. Gross P, deTreville RT, Cralley LJ, Granquist WT, Pundsack FL. The pulmonary response to fibrous dusts of diverse compositions. *Am Ind Hyg Ass J* 970;31:125-32.

15. Harrel S, Molinari J. Aerosols and splatter in dentistry: a brief review of the literature and infection control implications. *JADA* 2004;134:429-37.

16. Hearl FJ. Industrial hygiene sampling and applications to ambient silica monitoring. *J Expo Anal Environ Epidemiol.* 1997;7:279-89.

17. Horvath A. Significance of the surface of crystalline silicoginic dusts in experimental silicosis. *Acta Morphol Acad Sci Hung.* 1976;24:213-22.

18. Hunter D. The pneumoconioses. In *The diseases of occupations.* Boston, Little, Brown & Co., 1955;848-854.

19. International Agency for Research on Cancer (IARC). Monographs Database on Carcinogenic Risks to Humans. Website. www.iarc.fr/

20. Ireland AJ, Moreno T, Price R. Airborne particles produced during enamel cleanup after removal of orthodontic appliances. *AmJOrthod Dentofacial Orthop* 2003;124:683-6.

21. Korn M, Ndhlovu D. Surgical masks – effective protection against cytostatic aerosols? *Dtsch Med Wochenschr.* 1989;114:1785-8.

22. Lee K, et. al. Pulmonary response of rats exposed to titanium dioxide (TiO_2) by inhalation for two years. *Toxicology and Applied Pharmacology* 1983;79:179-192.

23. Linch KD. Respirable concrete dust – silicosis hazard in the construction industry. *Appl Occup Environ Hyg*. 2002;17:209-21.

24. Luchtel DL, Martin TR, Boatman ES. Response of the rat lung to respirable fractions of composite fiber-epoxy dusts. *Environ Res.* 1989;48:57-69.

25. Marple VA, Olson BA, Miller NC. The role of inertial particle collectors in evaluating pharmaceutical aerosol delivery systems. *J Aerosol Med* 11: :S139-S153

26. May KR. The Cascade Impactor: An Instrument for Sampling Coarse Aerosols. *J Sci Instrum* 1945;22:187-95.

27. Miller RL, Micik RE. Air pollution and its control in the dental office. *Dent Clin North Am* 1978;22:453-76.

28. Miller BG, Hagen S, Love RG, Soutar CA, Cowie HA, Kidd MW, Robertson, A. Risks of silicosis in coalworkers exposed to unusual concentrations of respirable quartz. *Occ and Env Med* 1998;55:52-58.

29. Mitchell JP, Costa PA, Waters S. An assessment of an Andersen Mark-II cascade impactor. *J Aerosol Sci.* 19:213-231

30. Mjor IA. *Dental Materials: Biological properties and clinical evaluations.* Boca Raton, CRC Pres, Inc., 1985;197-201.

31. National Toxicology Program: 9th Report on Carcinogens. U.S. Department of Health and Human Services, Public Health Service, Washington, DC 2000.

32. Newman R. Association of biogenic silica with disease. *Nutr Cancer* 1986;8:217-

221.

33. Oberg T, Brosseau LM. Surgical mask filter and fit performance. *Am J Infect Control.* 2008 May; 36(4):276-82.

34. O'Neill CH, Hodges GM, Riddle PN, Jordan PW, Newman RH, Flood RJ, Toulson EC. A fine fibrous silica contaminant of flour in the high esophageal cancer area of north-east Iran. *Int J of Cancer* 1980;26:617-628.

35. O'Neill CH, Pan Q, Clarke G, Liu F, Hodges G, Ge M, Jordan P, Chang U, Newman R, Toulson E. Silica fragments from millet bran in mucosa surrounding esophageal tumors in patients in northern China. *Lancet 1982;*29:1202-1206.

36. Pan G, Takahashi K, Feng Y, Liu L, Liu T, Zhang S, Liu N, Okubo T, Goldsmith DF. Nested case-control study of esophageal cancer in relation to occupational exposure to silica and other dusts. *Am J Ind Med* 1999;35:272-280.

37. Reynolds IR A review of direct orthodontic bonding. *Br J orthod 1975; 2:171-178.*

38. Reiser KM, Last JA. Silicosis and fibrogenesis: fact and artifact. *Toxicology 1979;*13:51-72.

39. Rose EF. Carcinogens and esophageal insults. *S Afr Med J 1968a;*42:334-336.

40. Rose EF. Phytolithicosis – A disease entity? *Trans NY Acad Sci 1968b;*30:1196-1200.

41. Shortall AC, Palin WM, Burtscher P. Refractive Index Mismatch and Monomer Reactivity Influence Composite Curing Depth. J Dent Res. 2008;87:84-88.

42. Soutar C, Robertson A, Miller BG, Searl A, Bignon J. Epidemiological evidence on the carcinogenicity of silica: factors in scientific judgement. *The Annals of occupational hygiene.* 2000;4: 3-14.

43. Stein SW, Olson BA. Variability *in size distribution measurements* obtained using

multiple Andersen Mark II cascade impactors. *Pharm Res.* 1997. 14:1718-1725.

44. Wallace WE, Harrison J, Keane MJ, Bolsaitis P, Eppelsheimer D, Poston J, Page SJ. Clay occlusion of respirable quartz particles detected by low voltage scanning electron microscopy analysis. *Ann Occup Hyg.* 1990 Apr;34(2): 195-204

45. Wozniak H, Goscicki J, Wiecek E. Experimental Silicosis. I. Fibrogenic activity of quartz material used in the ceramic industry. *Med Pr.* 1979; 30(5): 337-44

46. Yabuta J, Ohta H. Determination of free silica in dust particles: effect of particle size for the X-ray diffraction and phosphoric acid methods. *Ind Health.* 2003;41:249-59.